The kinetic characterization of mutated cyanobacterial dual-functioning fructose/sedoheptulose bisphosphate using a malachite green colorimetric assay

Author:
Albert Anis – albertannis@gmail.com

Supervisors:
PhD candidate Karen Schriever* - karensch@scilifelab.se
Assoc. Prof. Paul Hudson* - huds@kth.se
Assoc. Prof. Ed van Niel† - ed.van_niel@tmb.lth.se

Examiner:
Prof. Marie Gorwa-Grauslund† - marie-francoise.gorwa-grauslund@tmb.lth.se

*KTH Royal Institute of Technology
†Lund University, Faculty of Engineering LTH

June 2021

Acknowledgements

I would like to offer my sincere gratitude to my supervisor Karen Schriever for her dedication in helping me accomplish this work and Paul Hudson for giving me the opportunity to do my thesis in his research group.

Abstract

The increased human dependence on fossil-based fuels, industrial chemicals, and structural materials has caused a drastic increase in atmospheric CO_2 levels during the past 50 years. Consequences of this have been observed in the disruption of terrestrial and aquatic ecosystems. Bioengineering of photosynthetic organisms capable of converting CO_2 into biomass and value-added organic molecules provide a promising solution to the problem. However, faster CO_2 fixation rates are needed in order to meet industrial scale production capacities. Previously published studies have mainly focused on the overexpression of Calvin cycle enzymes or engineering of ribulose 1,5-bisphosphate carboxylase-oxygenase (RuBisCO) whereas fewer have looked into the engineering of enzymes downstream of RuBisCO. In this thesis, a malachite green-based colorimetric assay was optimized and used in characterizing the kinetic properties of wild type bifunctional cyanobacterial fructose/sedoheptulose bisphosphatase (cy-F/SBPase) and variants of the enzyme with respect to the hydrolysis of one of its substrates (fructose 1,6-bisphosphate). The assay was validated by successfully assaying a set of previously kinetically characterized cy-F/SBPase variants as well as the wild type. Subsequently, a group of rationally *de novo* designed mutants of the enzyme was kinetically characterized. This way, a crude understanding of new aspects of the protein structure-function relationship was established, which could potentially guide future protein engineering efforts on cy-F/SBPase. The developed malachite green assay could also complement such research efforts as a result of its multiplexed format which is desirable when assaying larger protein libraries.

1. Introduction

Photosynthesis comprises several biochemical pathways that are mainly prevalent in in algae, plants, and cyanobacteria. In simplified terms, photosynthesis can be described as the conversion of CO_2, H_2O, and light into O_2 and $C_6H_{12}O_6$ (Johnson, 2016). The carbohydrates and breathable oxygen generated as products of photosynthesis fuel all heterotrophic microbes and animals that rely on these resources. Rising atmospheric CO_2 levels from human industrial activity have resulted in the disruption of various ecosystems and extinction of animals and plants (Root et al., 2003) through rising sea levels (Nicholls, 2002), an increase in global temperature (Hansen et al., 2006) and acidification of oceans, seas, and lakes (Pandolfi et al., 2011) amongst other devastating effects. Some sources also point to more frequent abnormal weather events due to increased global temperature (Rosenzweig et al., 2001; Stott, 2016). An international collaborative study facilitated by the Global Carbon Project (Friedlingstein et al., 2020) estimates that the annual release of CO_2 has nearly doubled during the last 50 years (Figure 1).

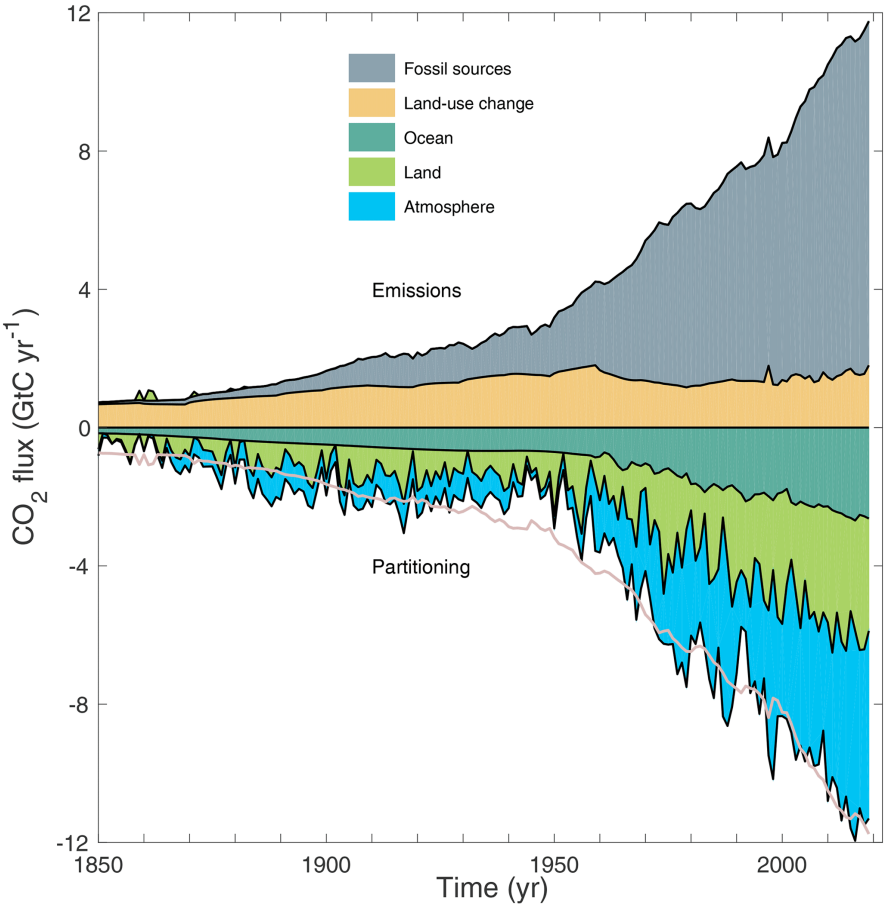

Figure 1 – The combined components of annual carbon release between 1850 and 2020 for fossil resources and change in land-use. The negative values correspond to their partitioning in land, oceans, and the atmosphere.

Looking from a population perspective, a forecast by the United Nations (2019) estimates that global population could reach 9.1 billion by 2050. If this estimation applies for the upcoming decades, an increase in global population will naturally be accompanied by an even higher demand for industrially produced goods such as fuels, commodity chemicals and construction materials. Hence, there is a clear need for more efficient carbon fixation and conversion strategies that can accelerate the transition to a biobased economy where emphasis is moved from raw materials sourced from fossil fuels to sustainable alternatives. The field of biotechnology has emerged as a promising solution for enabling this transition (Soetaert & Vandamm, 2006). Discoveries in gene technology and protein and metabolic engineering have paved the way in the engineering of novel plants and microorganisms capable of generating useful carbon-based resources such as fuels, foods, medicine, and industrial polymers (Bhatia & Goli, 2018). Since atmospheric CO_2 is not only an undesired pollutant but also highly abundant, extensive research has been performed focusing on various approaches of utilizing it as a starting material to produce the previously mentioned chemicals on an industrial scale (Gong et al., 2018). Plants, algae, and cyanobacteria with their inherent ability of fixating and converting CO_2 through photosynthesis represent suitable host organisms for sustainable biomanufacturing.

1.1 Photosynthesis

Photosynthesis is composed of two main biochemical reaction cascades: the light-dependent reactions and the Calvin cycle (sometimes referred to as the light independent reactions) which are connected via shared metabolites. In the light-dependent reaction chlorophyll pigments are excited by photons and release electrons. These electrons are passed along a series of enzymes that together make up the electron transport chain (ETC) which is located along the thylakoid membrane. The electrons are used to reduce $NADP^+$ into NADPH which is an essential co-factor in the Calvin cycle. Released electrons are replenished through the oxidation of two H_2O molecules into $4H^+$, O_2 and $4e^-$, which eventually causes a build-up of excess protons inside the thylakoid. The resulting proton gradient across the thylakoid membrane drives the ATP synthase membrane protein to channel excess protons out of the thylakoid in a set of rotary motions, which enable ATP synthesis (Amesz, 1987).

The Calvin cycle is responsible for fixing and converting CO_2 into carbohydrates. It is not dependent on light and is therefore also referred to as the “light-independent reactions” or “dark reactions” of photosynthesis. Instead, it depends on the chemical energy from ATP and the reducing power of NADPH which are both provided from the light-dependent reactions. A scheme of the cycle can be viewed in Figure 2.

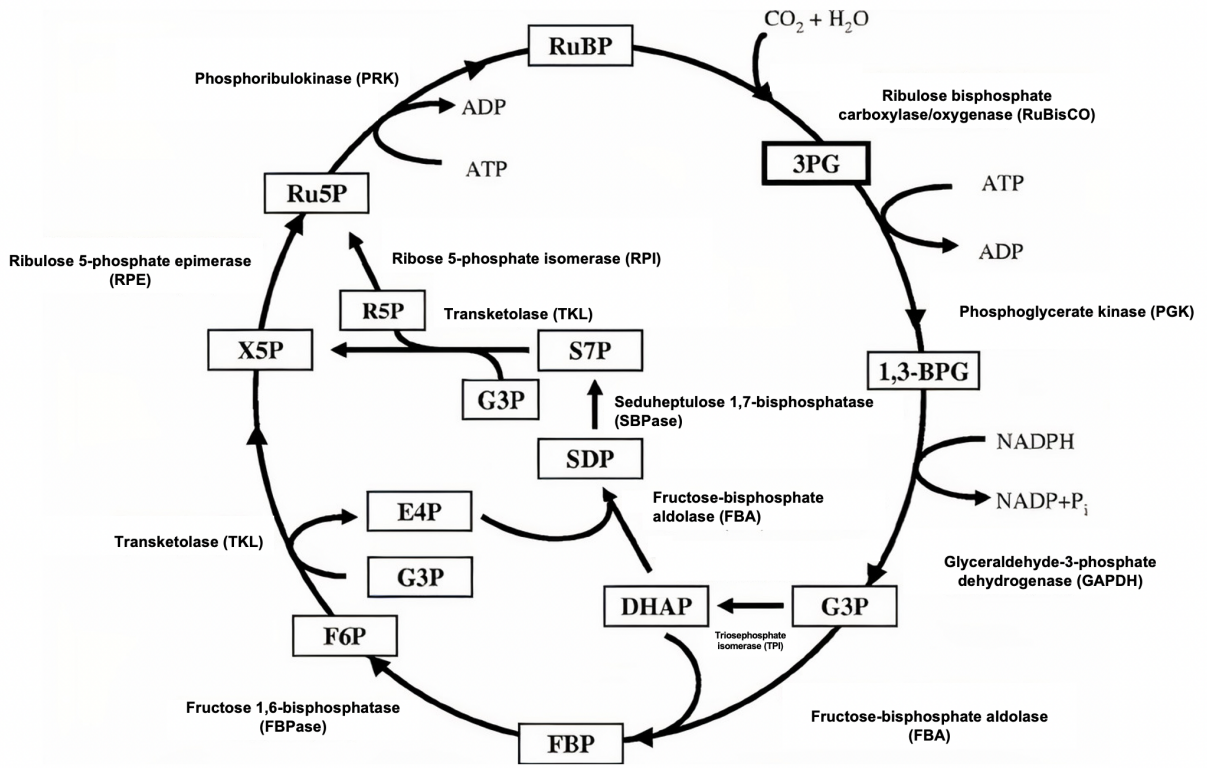

Figure 2 - The Calvin cycle. Abbreviations: 3PG, 3-phosphoglycerate; 1,3-BPG, 1,3-bisphosphoglycerate; G3P, glyceraldehyde 3-phosphate; DHAP, dihydroxy-acetone-phosphate; SDP, sedoheptulose 1,7-bisphosphate; S7P, sedoheptulose 7-phosphate; E4P, erythrose 4- phosphate; FBP, fructose 1,6-bisphosphate; F6P, fructose 6-phosphate; R5P, ribose 5-phosphate; X5P, xylulose 5-phosphate; Ru5P, ribulose 5-phosphate; RuBP, ribulose 1,5-bisphosphate. Figure and abbreviations list is adapted from (Wang et al., 2011)

The cycle can roughly be divided into three phases: carboxylation of ribulose 1,5-bisphosphate (RuBP), reduction of 1,3-bisphosphoglycerate and regeneration of RuBP. Each turn of the cycle incorporates one CO_2 molecule; hence taking six turns of the cycle to generate a complete hexose sugar. Carboxylation is facilitated by the enzyme ribulose bisphosphate carboxylase/oxygenase (RuBisCO) and is highly exergonic meaning that the reaction is practically irreversible (Blankenship, 2002). It facilitates a series of reactions leading to the breakdown of RuBP into two molecules of 3-phosphoglycerate (3PG). A wasteful side reaction of RuBisCO called oxygenation can occur during this step and become a bottleneck in the cycle. When this happens

RuBP reacts with O_2 instead of CO_2, resulting in one molecule of 3PG and 2-Phosphoglycolate (2PG). Three carbons from two molecules of 2PG are recovered by a salvage pathway and in turn release one CO_2 molecule through a process called photorespiration. Photorespiration is wasteful because organic carbon is converted into CO_2 without the production of ATP or NADH (Blankenship, 2002). Moving along the cycle, carboxylation of RuBP is then followed by phosphorylation and reduction of 3PG into glyceraldehyde 3-phosphate which is then isomerized into dihydroxy-acetone-phosphate. A subset of generated G3P molecules exits the Calvin cycle when the level of cycle metabolites is sufficient to produce sucrose or starches via other metabolic pathways whilst a majority of G3P is returned back into the cycle to form RuBP in the so-called regeneration phase(Johnson, 2016)

1.2 Engineering of the Calvin cycle

In contrast to using plants and algae as biological cell factories, cyanobacteria offer certain physiological and practical advantages in an industrial context where high product yields are important. Cyanobacteria grow faster and can use atmospheric N_2 as a nitrogen source. Another advantage is the wider range of available genetic tools for the organism which enable rapid experimental prototyping (Rosgaard et al., 2012). A series of value-added chemicals such as ethanol, isobutanol, glycerol and fatty acids have been successfully produced by introducing biosynthetic pathways in cyanobacteria (Knoot et al., 2018). Despite these achievements, the main challenge remaining is low yields (Rosgaard et al., 2012) which might be circumvented by modifying and/or upregulating the enzymes involved in operating the Calvin cycle with some identified potential enzyme engineering candidates. The most common candidate in both plants and cyanobacteria has been RuBisCO due to it being the key responsible enzyme for organismal CO_2 fixation. Even though numerous approaches have been primarily aimed at mitigating its oxygenation reaction or increase its carbon fixation rate, significant improvements have not been achieved this far (Durall & Lindblad, 2015). Other potential targets for enzyme upregulation or engineering targets have been those involved in the regeneration of RuBP that exhibit metabolic limitations over the cycle in cyanobacteria and plants (Janasch et al., 2018; Liang & Lindblad, 2016; Ma et al., 2007). Individual overexpression of pathway enzymes known to exhibit metabolic control such as transketolase (TKA), fructose-bisphosphate aldolase (FBA)

and fructose 1,6/sedoheptulose 1,7-bisphosphatase (F/SBPase) all showed to increase cell dry weights by 50-60% in *Synechocystic* sp. PCC 6803 (Liang & Lindblad, 2016). Similar results have been achieved in plants by upregulating non-RuBisCO enzymes in the Calvin cycle (Tamoi et al., 2006). Another overexpression study in *Synechococcus* sp. PCC 7002 showed that upregulating F/SBPase expression not only led to increased growth capacities but also a global reprogramming of carbon metabolism towards non-storage carbohydrates (de Porcellinis et al., 2018). This feature, besides the ability of increasing biomass, could potentially also be used to direct the carbon flow towards desired metabolites.

2. Aim

While overexpression of non-RuBisCO Calvin cycle enzymes has previously been demonstrated to improve growth rate and biomass yields, few efforts have been made at rationally engineering of said enzymes from cyanobacteria to improve their catalytic properties. In this thesis, cyanobacterial F/SBPase from *Synechocystis* sp. PCC 6803 (referred to as cy-F/SBPase) was engineered and assayed to study the phenotypic effects certain point mutations have on catalytic activity, ligand binding and redox regulation.

The first sub-aim of this thesis was to systematically optimize a protocol for a colorimetric assay to study cy-F/SBPase activity towards one of its substrates (fructose 1,6-bisphosphate) *in vitro*. In order to assess the accuracy of the assay, six single residue exchange variants (referred to as the *validation set*) published by Feng et al (2014) were used for validating the accuracy of the assay. The second sub-aim consisted of characterizing the kinetic parameters of a set of 8 rationally designed point mutations (referred to as the *test set*) which have not been previously described.

3. Background

3.1 F/SBPase structure, function, role

Cyanobacterial F/SBPase from *Synechocystis* sp. PCC 6803 is a tetrameric protein (Figure 3) composed of four identical subunits (C1-C4). Each monomer is approximately 39 kDa and contains a substrate binding site as well as an allosteric site (Hu et al., 2011). The active site which is slightly buried in the protein structure requires Mg^{2+} to stabilize the microenvironment around the active site residues in order to enable substrate binding (Sun et al., 2012).

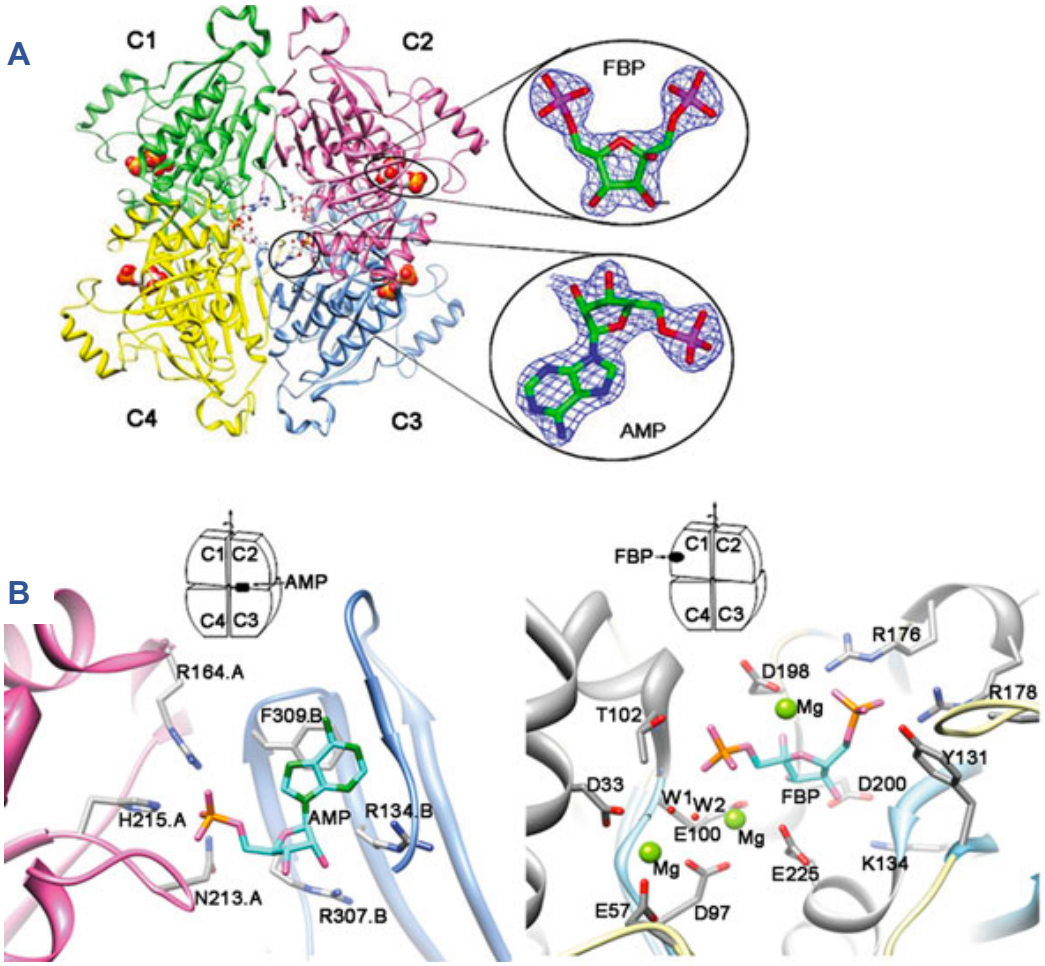

Figure 3 – A) A cartoon representation of cyanobacterial F/SBPase in complex with FBP and its allosteric inhibitor AMP. B) The location of the AMP allosteric site (left panel) and the substrate binding site (right panel) with the amino acids, Mg^{2+} and water molecules involved with ligand interaction. The backbone of one protein subunit is shown in red cartoon whereas the backbone of the adjacent subunit is shown in blue. Side chains of residues directly involved in ligand binding are shown as sticks. Mg^{2+} are shown as green spheres.

The allosteric site is located between the interfaces of two subunits and has a strong affinity to adenosine monophosphate (AMP) which acts as an inhibitor. The enzyme is a dual functioning enzyme in cyanobacteria (Jiang et al., 2012) that is responsible for both converting FBP into fructose 6-phosphate (Figure 4) and sedoheptulose 1,7-bisphosphate into sedoheptulose 7-phosphate (Figure 5), which are reactions usually catalyzed by two different enzymes in most carbon-fixating organisms (Johnson, 2016). In this study however, only the FBPase activity of cy-F/SBPase towards its substrate FBP was studied.

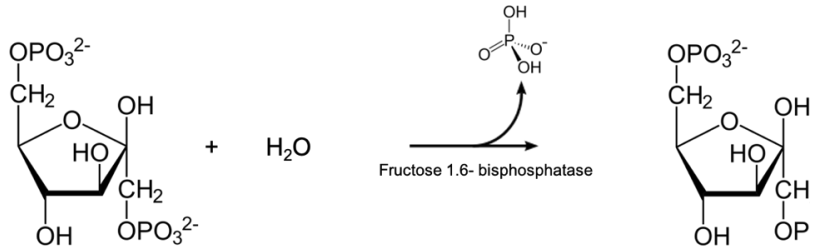

Figure 4 - The hydrolysis of fructose 1,6-bisphosphate by fructose 1.6-bisphosphatase

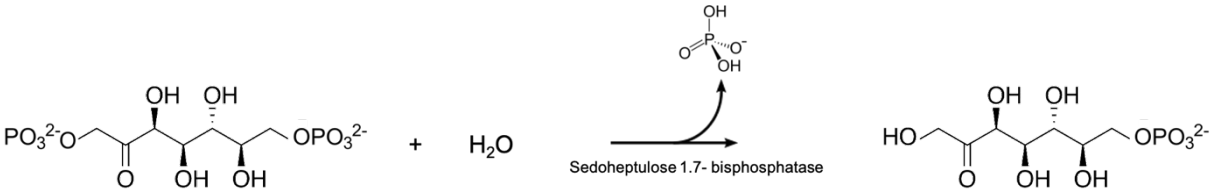

Figure 5 – The hydrolysis of sedoheptulose 1,7-bisphosphate by sedoheptulose 1.7-bisphosphatase

Besides the active and allosteric sites there is another important domain in the cy-F/SBPase enzyme. Mutagenesis studies suggest that a disulfide bridge may form between residues C75 and C99, stabilizing the non-active initial state of the enzyme which gets disrupted at reducing conditions (Feng et al., 2014). In an experimental setting the reducing agent dithiothreitol (DTT) is employed to mimic the ferredoxin/thioredoxin system found naturally in cyanobacteria (Gütle et al., 2016). A potential connection between the active site and the regulatory site has been proposed by Feng et al (2014) and is shown in Figure 6.

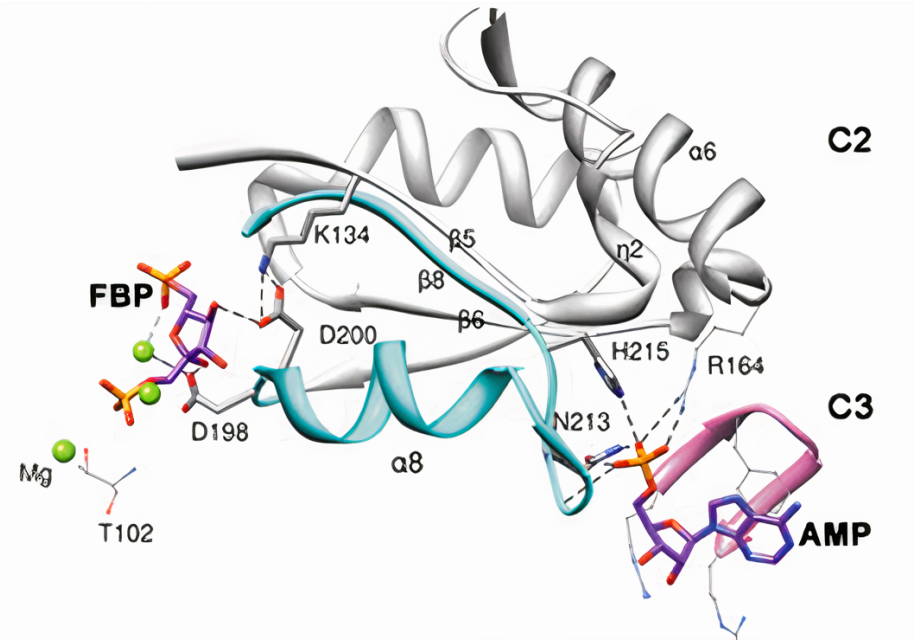

Figure 6 – The proposed linkage between the AMP and FBP binding sites by Feng et al (2014). The loop in blue cartoon composed of α8β8 might be involved in transducing allosteric signaling between N213 and H215 to D198 and D200. The loop in white cartoon composed of α6η2β5β6 might be involved in transducing allosteric signaling between R164 and K134.

Based on kinetic and structural analysis in the absence and presence of AMP, Feng et al proposed that residue R164 and H215 that are involved in AMP binding at the allosteric site may undergo long-range interactions with D198, D200 and K134 which are located within or in proximity to the substrate binding site. The authors suggests that this allosteric signaling may be transmitted from N213 and H215 to D198 and D200 through the blue loop in Figure 6 composed of α8β8 while signaling between R164 and K134 may be transmitted through the white loop α6η2β5β6.

3.2 Enzyme kinetics

Enzyme kinetics is the quantitative description of chemical reactions catalyzed by enzymes. In most cases, enzyme kinetics can be described by the Michaelis-Menten equation (Equation 1) (Berg et al., 2015). The model describes enzymatic reactions that transition from enzyme and substrates to enzymes and products as occurring in two steps. At first, an enzyme-substrate complex is formed in a reversible manner which is followed by irreversible reaction where the substrate is converted into product.

Equation 1

$$v_0 = \frac{V_{max} \times [S]}{K_M + [S]}$$

The reaction rate (formation of product per unit of time) is depicted as v_o. The substrate concentration is depicted as [S]. V_{max} is the maximum reaction rate at saturated substrate levels. The maximum reaction rate can also be expressed as $k_{cat} \times [E]$ where the constant k_{cat} is the turnover number describing the number of substrate-to-product formations that occur per unit of time and *[E]* is the enzyme concentration. The Michaelis constant K_M describes the substrate concentration where v_0 equals half of V_{max} (Berg et al., 2015). The model describes that enzyme activity increases in a linear fashion together with substrate concentration until all of the enzyme molecules are saturated (Equation 1). After this point the reaction rate stagnates as any additional increase in substrate will not have an effect on it (Berg et al., 2015).

Despite its utility in describing many types of enzymes adequately, this model represents a simplified description of enzymatic behavior and does not account for multimeric enzymes containing more than one catalytic site that affect one another. Cy-F/SBPase has 4 catalytic sites where FBP can be converted to its product. The Hill-Langmuir function (Equation 2) can be applied to account for subunit cooperativity (Alon, 2007).

Equation 2

$$v_0 = \frac{V_{max} \times [S]^n}{{K_M}^n + [S]^n}$$

The added parameter *n* is the Hill-coefficient and determines the extent of the sigmoidal shape of the plotted curve. An *n*-value greater than 1.0 indicates positive cooperativity whereas a value less than 1.0 indicates negative cooperativity (Berg et al., 2015). Since V_{max} is equivalent to $k_{cat}[E]$, Equation 2 can be rewritten as Equation 3 to express the reaction rate in time (s^{-1}).

Equation 3

$$\frac{v_0}{[E]} = \frac{k_{cat} \times [S]^n}{{K_M}^n + [S]^n}$$

This equation form was used in this thesis as it streamlines the calculation of k_{cat}, K_M, and n. It also makes kinetic data easier to understand by not having to know the underlying enzyme concentration used in the assay.

3.3 Colorimetric enzyme assays

Kinetic assays for enzymes usually measure the rate of either substrate consumption or product formation (Bisswanger, 2014). This is done in order to determine the kinetic characteristics of an enzyme towards its substrate by then fitting the measured data to a proposed model such as the Michaelis Menten equation or the Hill equation as mentioned in section 3.1.

A wide range of techniques and assays are used in characterizing the catalytic properties of enzymes (Purich, 2010). One commonly applied approach is the use of absorption spectroscopy due to the accessibility of spectrophotometric equipment in common research laboratories. The sample is illuminated by light within the visible and ultraviolet spectrum and the intensity of the incident and transmitted light is registered by the spectrophotometer. The spectrophotometer converts these readings into absorbance units based on the Beer-Lambert Law in Equation 4:

Equation 4

$$\Delta Abs = log\frac{I_0}{I} = \varepsilon \times \Delta c \times l$$

where ΔAbs is the absorbance, $\boldsymbol{I_0}$ and $\boldsymbol{I}$ are the incident and transmitted intensities, ε being the molar absorption coefficient that is unique for every analyte, c is the concentration of the sample, and l is the pathlength of the cuvette(Purich, 2010).

There are two types of colorimetric assays: continuous and discontinuous. Continuous assays directly measure the production formation or substrate consumption in real time and rely on either substrate or product being colorimetric themselves. In a discontinuous assay, a sample from the enzyme reaction is quenched during or before it is added to a development solution containing reagents that complex the analyte to produce a colorimetrically detectable compound. In this project, a discontinuous malachite green (MG) colorimetric assay was adapted from Vardakou et al (2014) to measure the kinetics for the conversion of FBP to fructose 6-phosphate by cy-F/SBPase and variants thereof. As shown in Figure 4, FBP releases one molar equivalent of orthophosphate (P_i) for each molar equivalent of FBP that is consumed in the enzymatic reaction. The substrate consumption rate can thus be determined by the indirect measurement of P_i through the MG assay. The MG development solution consists of $(NH_4)_2MoO_4$, MG oxalate salt, Tween20 and H_2SO_4. The development solution fulfils two roles. The first one is to quench the enzymatic reaction by lowering the pH and thus rendering the enzyme inactive. The other function is to form a complex with P_i that can be measured spectrophotometrically. When adding a sample from the enzymatic reaction, released P_i reacts with $(NH_4)_2MoO_4$ under acidic conditions and forms a molybdate-P_i species ($(NH_4)_3PO_4Mo_{12}O_{36}$), NH_4^+ and H_2O according to Reaction 1.

Reaction 1

$$PO_4^{3-} + 12(NH_4)_2MoO_4 + 24H^+ \rightarrow (NH_4)_3PO_4Mo_{12}O_{36} + 21NH_4^+ + 12H_2O$$

The reaction sequence continues by MG oxalate reacting with the formed molybdate-P_i to form a MG-molybdate-P_i complex according to Reaction 2 that can be detected spectrophotometrically at 620-650 nm (Baykov et al., 1988).

Reaction 2

$$(NH_4)_3PO_4Mo_{12}O_{36} + MG \rightarrow \frac{MG \cdot H_2PO_4(MoO_3)_{12}}{\lambda_{620-650}} + 3NH_3$$

Tween 20, also known as polysorbate, is included in the development solution as it helps stabilizing the MG-phosphomolybdate complex at P_i concentrations above 10 µM (Baykov et al., 1988).

3.4 Engineering of F/SBPase in this project

Two sets of cy-F/SBPase variants were studied in this project. First, a set that was assembled based on published variants from Feng et al (2014) – denoted as the *validation* set – was used to validate the colorimetric assay that was developed. The second set was denoted as the *test* set and contained a selection of cy-F/SBPase variants that were designed *de novo* by Karen Schriever based on rational considerations. Both sets of variants are discussed below. Due to the scope and time frame of this thesis, only the FBPase activity of cy-F/SBPase variants towards fructose 1.6-bisphosphate as substrate was studied.

Validation set cy-F/SBPase variants

The test set variants were selected among a list of published variants (Feng et al, 2014), so that different effects of residue exchanges on catalysis and substrate affinity, redox regulation and allosteric control were represented. Specifically, T102A, R176A and K134A that are located at or close to the active site (as shown in Figure 7) were shown to impact substrate affinity and catalysis (Feng et al, 2014). Variant K29A was the only variant that was described by Feng et al. for which an increase in turnover number k_{cat} was observed (from 10.5 s^{-1} to 21.3 s^{-1}).

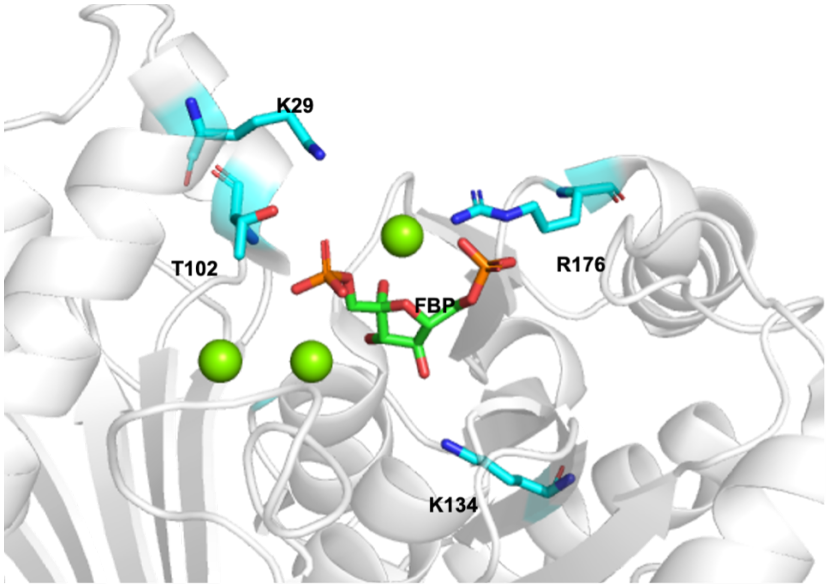

Figure 7 – The substrate binding site of one Cy-F/SBPase monomer is shown as gray cartoon (PDB ID: 3rpl). Active site residues of cy-F/SBPase that are exchanged in T102A, R176A and K134A variants are shown as cyan sticks together with the bound substrate FBP and Mg^{2+} as green spheres.

Another variant that was included in the *validation set* was C75S. According to Feng et al (2014), C75 likely is an important player in redox regulation of cy-F/SBPase by forming a disulfide bridge with C99 that stabilizes the inactive state in an oxidative environment. Exchanging this residue to serine appears to disrupt this disulfide bridge, thereby removing the need of using the reducing agent dithiothreitol (DTT) in order for the enzyme to efficiently catalyze FBP hydrolysis.

A final variant that was included in the *validation set* was R307A. The side chain of R307 is directly involved in AMP binding (Figure 8) and exchanging it to the small amino acid alanine consequently diminishes AMP-mediated allosteric inhibition which results in a drastic increase of the half maximal inhibitory concentration (IC_{50}) from 32 µM to above 10000 µM AMP in comparison to the wild type (Feng et al., 2014).

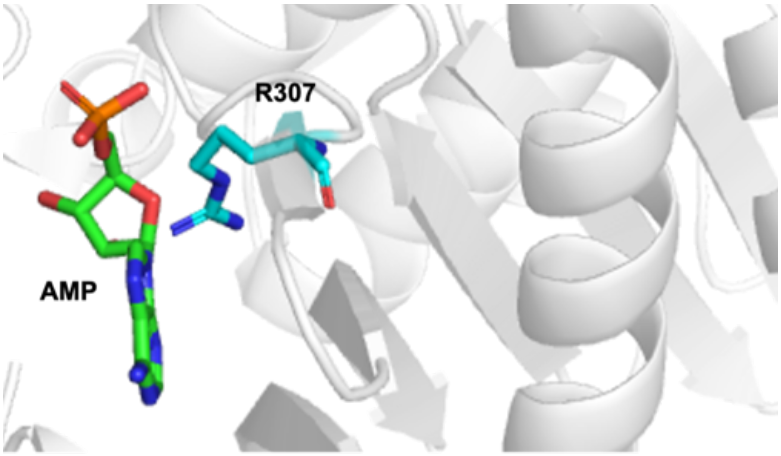

Figure 8 - The allosteric site of one cy-F/SBPase monomer is shown as gray cartoon (PDB ID: 3rpl). The allosteric site residue R307 is shown as cyan sticks together with the bound allosteric inhibitor AMP in green sticks.

Test set cy-F/SBPase variants

A set of eight cy-F/SBPase variants that have not previously been described were characterized in order to gain further insight into the structure-function relationship of the enzyme, focusing mainly on the transmissibility of allosteric inhibition signal.

Three of these variants – A216V, M218I and G219V – represent residue exchanges that modify the hydrophobic core between the β-sheet and α-helix that connect the allosteric and substrate binding sites and therefore may impact transmissibility of the allosteric inhibition signal (Figure 9). A turn that directly connects the respective β-sheet and α-helix is formed by two rigid proline residues. The P138A exchange variant was included in the test set in order to assess if the structural integrity of this turn is essential for enzyme activity.

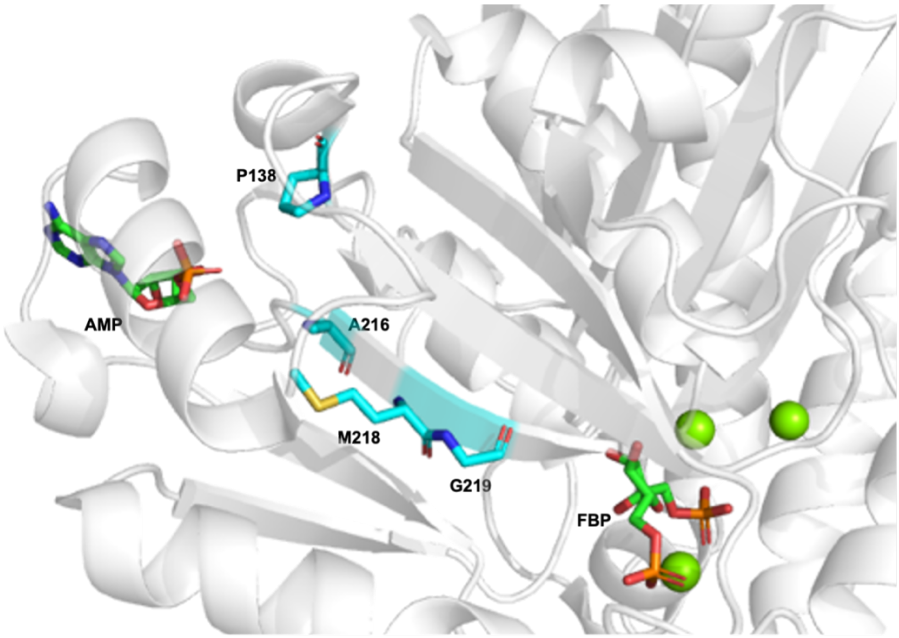

Figure 9 – The substrate binding site and allosteric site of one cy-F/SBPase monomer are shown as gray cartoon (PDB ID 3rpl). Residues that are discussed in the main text are shown as cyan sticks together with the bound allosteric inhibitor AMP and substrate FBP in green sticks and Mg^{2+} as green spheres.

Variants R192N and R194H were included in order to evaluate transmission of AMP allosteric signal via potential interactions with N213 (Figure 10) that was previously shown to be involved with AMP binding (Feng et al., 2014). Moreover, residue K134 was previously shown to be important for allosteric transmission to the active site as reflected in the increase of IC_{50} from 34 μM to 2099 μM AMP in comparison to the wild type (Feng et al, 2014) despite this residue being located quite far away from the allosteric binding site. The residue exchange K134N was included in order to observe if activity and allosteric transmission could be maintained when mutating to a non-basic, smaller residue that is capable of hydrogen bonding.

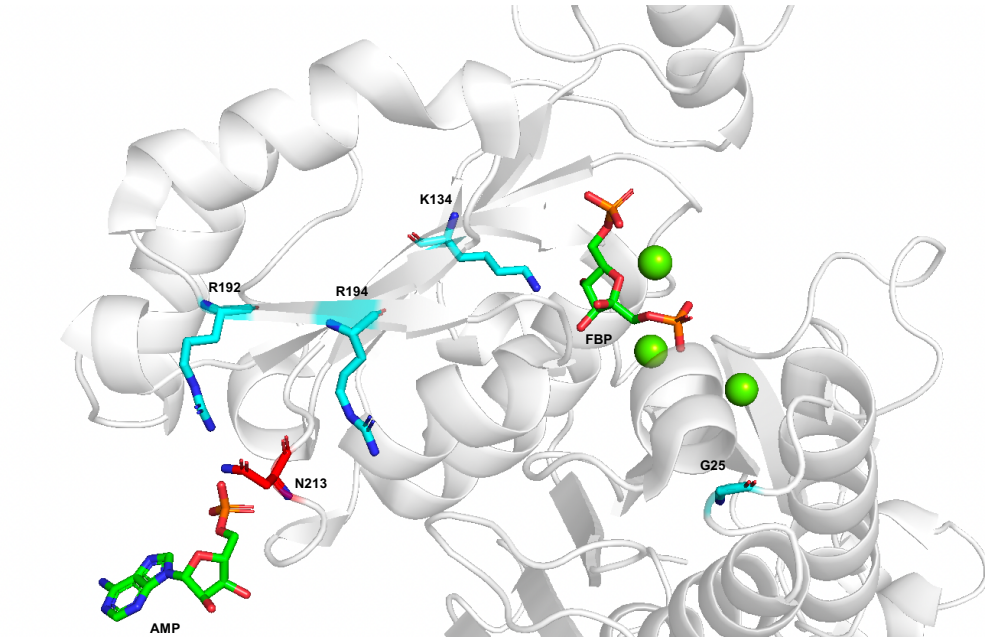

Figure 10 – The substrate binding site and allosteric site of one cy-F/SBPase monomer are shown as gray cartoon (PDB ID: 3rpl). Residues that are discussed in the main text are shown as cyan sticks together with the bound allosteric inhibitor AMP and substrate FBP in green sticks and Mg^{2+} as green spheres.

Finally, a G25A variant was included to study its effect on enzymatic activity based on the premise that G25 may control the flexibility of the loop that positions K29 with respect to the active site, with a K29A exchange previously shown to double k_{cat} (Feng et al. 2014)

4. Materials and Methods

4.1 Host strains

Two bacteria host strains were used in this project: an *Escherichia coli (E. coli)* XL1-Blue strain (Stratagene) for subcloning due its high competency in yielding high-quality plasmid DNA (Chan et al., 2013) and an *E. coli* BL21(DE3) strain (Merck) as it allows efficient protein expression for genes under control of a T7 promoter (Rosano & Ceccarelli, 2014).

Chemically competent XL1-Blue and BL21(DE3) cells were prepared by plating a frozen glycerol stock of the culture on a petri dish with nutrient agar (Merck) that was incubated 16 hours (overnight) at 37 °C. A pre-culture was prepared by inoculating 10 ml lysogeny broth (LB) (10 g/l Tryptone, 5 g/l yeast extract, 5 g/l NaCl) with a single colony. The pre-culture was incubated at 37 °C and 200 revolutions per minute (rpm) overnight. Subsequently, 1 l of LB medium was inoculated with the entire volume of the pre-culture and cultivated at 37 °C and 200 rpm until an optical density at 600 nm (OD_{600}) of 0.35-0.4 was reached. The culture was thereafter immediately chilled on ice for 30 min and swirled occasionally. The cells were split into four tubes and pelleted by centrifugation at 3000 xg for 15 min at 4 °C. Each pellet was carefully resuspended in 100 ml chilled 100 mM $MgCl_2$, pooled together in a centrifuge bottle and centrifuged once more at 2000 xg for 15 min at 4 °C. The resulting pellet was washed with 200 ml pre-chilled 100 mM $CaCl_2$ and harvested at 2000 xg for 15 min at 37 °C. The supernatant was decanted and the pellet was resuspended in 50 ml of ice cold 85 mM $CaCl_2$ in 15% v/v glycerol. Cells were centrifuged at 1000 xg for 15 min at 4 °C and the supernatant was discarded. The cells were finally resuspended in 2 ml of ice cold 85 mM $CaCl_2$ in 15% v/v glycerol per liter of culture, aliquoted into sterile tubes and flash frozen using liquid N_2. Competent cells were stored at -80 °C until use.

4.2 Genetic constructs

All cy-F/SBPase variants in this project were cloned into a pET28a(+) expression vector from Merck Millipore. Amongst its many features the ones most relevant for this project comprise an IPTG (Isopropyl β-D-1-thiogalactopyranoside)-inducible T7 promoter, a multiple cloning site, a kanamycin resistance marker and an N-terminal

6xHis tag. The gene sequences for all cy-F/SBPase mutants in this project were ordered (Twist Biosciences) as codon-optimized gene fragments. Each construct was flanked by standardized 5' and 3' gene synthesis adapters as provided by the manufacturer. This allowed the use of the same forward and reverse primers (Table A1) for amplification by polymerase chain reaction (PCR).

4.3 Subcloning

Transformation

The pET28a(+) expression vector was amplified in *E. coli* XL1-Blue cells. The plasmid was transformed into chemically competent cells using a standard heat-shock protocol. In brief, 1 µl purified plasmid solution (equivalent to 10 ng) was incubated with the cells on ice for 30 min. Cells were heat shocked at 42 °C for 45 sec in a water bath and then immediately chilled on ice for 2 min. Subsequently, the cells were subjected to a recovery incubation phase of 1 hour at 37 °C and 200 rpm in antibiotic-free LB medium (450 µl per 50 µl cells). Cells were concentrated to 200 µl by centrifugation at 1000 xg for 5 min and 100 µl of the cell suspension was plated on nutrient agar plates containing 50 µg/ml kanamycin. The plates were incubated overnight at 37 °C and stored at 4 °C until use.

Plasmid extraction

Single colonies from the transformation were transferred into 7 ml of LB-media (50 µg/ml kanamycin, freshly added) and incubated at 37 °C and 200 rpm overnight. The pre-culture was harvested by 15 min centrifugation at 4 °C, 3800 xg. The pET28a(+) plasmid was extracted from the cell pellet using the GeneJET Plasmid MiniPrep kit (ThermoFisher Scientific) according to the manufacturer's instructions with a few exceptions; after the wash step the spin column was centrifuged for 2 min instead of 1 min to ensure that all of the wash solution exits the membrane. Elution was performed using 30 µl of filtered dH2O after a 5 min incubation time with the column. Plasmid concentration was then measured spectrophotometrically on a NanoPhotometer NP80 (Implen).

Gene amplification

Each cy-F/SBPase variant construct was amplified by PCR. The PCR mix was prepared using the Phusion High-Fidelity PCR (ThermoFisher Scientific). Each PCR reaction contained a final composition of 1x Phusion HF Buffer, 0.2 mM dNTP, 0.5 µM each of forward and reverse primer (sequence given in Table A1), 1 ng/µl template DNA and 0.02 U/µl Phusion DNA polymerase. The PCR reaction was incubated at 98 °C for 30 sec to preheat the sample, 30 cycles consisting of 98 °C for 10 sec, 50 °C for 30 sec and 72 °C for 15 sec and a post-incubation period of 8 min at 72 °C. The resulting reaction mix was analyzed by gel electrophoresis on a 1% agarose gel stained with GelRed (VWR) which was run at 200 V for 20 min. DNA concentration was measured on the NanoPhotometer NP80.

Restriction and DNA purification

Cy-F/SBPase variant gene fragments and the pET28a(+) plasmid were digested using FastDigest *XhoI* and *NdeI* restriction enzymes (ThermoFisher Scientific). For the gene fragments 1 µg of DNA was incubated with 1 µl of each restriction enzyme, 2 µl FastDigest Green 10x buffer and the final reaction volume was adjusted to 20 µl using filtered dH2O. For the restriction of pET28a(+) 2 µg of DNA was used and the reaction mix was scaled accordingly. Restriction reactions were performed at 37 °C on a heating block for 2 hours. To verify that the restriction worked, 1 µl of the restriction mixtures were loaded onto a 1% agarose gel. Upon complete restriction, 1 µl of FastAP alkaline phosphatase (ThermoFisher Scientific) was added exclusively to the plasmid restriction reaction, in order to remove 5’ phosphate groups and prevent self-ligation, and the reaction was left to incubate for an additional 15 min. Restricted DNA mixes were purified by gel electrophoresis on a preparative 1% agarose gel and the correct bands were excised with a scalpel underneath a UV-lamp. Extraction of DNA from the gel slice was performed using the GeneJET gel extraction kit (ThermoFisher Scientific) according to the manufacturer’s instructions with the same minor modifications as when purifying PCR products. Both the insert and plasmid were purified from the same gel due to the fact that the exact composition of the gel may have an impact on the pH and salt content of the purified DNA samples, which in turn may affect ligation efficiency if it differs between vector and insert.

Ligation

Ligation of the restricted gene fragments into pET28a(+) was performed using a 3:1 molar ratio of insert to plasmid. A total of 100 ng of pET28a(+) and 55 ng of FBPase insert were mixed with 2 µl of 10x T4 DNA ligase buffer and 0.5 µl of T4 DNA ligase in a total reaction volume of 20 µl. The sample was left to incubate on the benchtop overnight at room temperature. The following day, 4 µl of ligation product were transformed into 50 µl competent *E. coli* XL1-Blue cells using the same transformation procedure as previously described and plated on nutrient agar plates with 50 µg/ml kanamycin. One colony from each plate was added to 7 ml of LB media with 50 µg/ml kanamycin (freshly added) and incubated at 37 °C and 200 rpm overnight. Cell cultures were harvested by centrifugation at 3800 xg and pET28a(+) including the FBPase gene of interest was purified using the GeneJET Plasmid MiniPrep kit according to the previously mentioned procedure. The DNA concentration was quantified using the NanoPhotometer NP80. Finally, the sequence of the gene inside the plasmid backbone was confirmed through sequencing by Eurofins Genomics using the sequencing primer in Table A1.

4.4 Protein expression

All of the sequenced pET28a(+)-F/SBPase constructs were transformed into *E. coli* BL21(DE3) using 10 ng of DNA according to the transformation protocol mentioned above. Overnight cultures were then set up by inoculating 10 ml LB (50 µg/ml kanamycin added freshly) with a single colony from each transformed construct respectively and incubating at 37 °C and 200 rpm. An expression culture consisting of 100 ml for the wild type and 50 ml for the validation and test set variants was prepared using rich media (2YT, 16 g/l tryptone, 10 g/l yeast extract, 5 g/l NaCl, 50 µg/ml kanamycin freshly added) and inoculated with the pre-culture to a final OD_{600} of 0.05. Cells were grown at 37 °C and 200 rpm to an OD_{600} of 0.4-0.6 at which the cells were induced using 0.5 mM IPTG for 5-6 hours at 37 °C and 200 rpm. Cells were harvested by centrifugation at 3800 xg and 4 °C for 20 min. The supernatant was discarded and the pellet was stored at -20 °C.

4.5 Protein purification

Validation set

Wild-type cy-F/SBPase and *validation set* variants were purified by immobilized metal ion affinity chromatography in a 96-well plate format using a His MultiTrap FF plate (Cytiva). Each well in the plate is packed with a stationary phase consisting of cross-linked agarose resin charged with Ni^{2+} ions that bind to histidine-tagged proteins. Prior to protein purification, each cell pellet was resuspended in 600 µl of lysis buffer (B-PER bacterial protein extraction reagent (ThermoFisher Scientific), 20 mM imidazole added) and incubated at 25 °C and 750 rpm for 20 min. The lysate was centrifuged at 3800 xg, 4 °C for 20 min. The supernatant representing the soluble fraction of the bacterial lysate was collected. The plate was equilibrated according to the manufacturer's instructions using wash buffer (50 mM Tris pH 8, 500mM NaCl, 20 mM imidazole). Each equilibrated well was loaded with 600 µl of the soluble fraction and the plate was incubated on a rocking bed shaker for 15 min. The plate was then centrifuged for 4 min at 100 xg to remove the flow through. Prior to eluting the protein, the plate was washed three times with 500 µl wash buffer and centrifuged at 500 xg for 2 min at 4 °C. Finally, the protein was eluted by adding 160 µl of elution buffer (50 mM Tris pH 8, 500 mM NaCl, 300 mM imidazole) and gently pipetting each well for 1 min to mix the buffer with the resin prior to centrifuging at 500 xg for 2 min at 4 °C. The flow-through and the first two elution fractions were analyzed by SDS-PAGE (sodium dodecyl sulphate–polyacrylamide gel electrophoresis) on a 4-15% polyacrylamide pre-cast gel (Bio-Rad) at 200V for 30 min to confirm protein expression and that the protein had eluted from the stationary phase. The gel was then stained with Coomassie Brilliant Blue dye and destained using dH_2O.

Eluted protein fractions were then buffer exchanged into storage buffer (20 mM Tris pH 8) using a PD MultiTrap G-25 plate (Cytiva). Each well on the plate contains a cross-linked dextran gel that retains smaller molecules such as salts, which therefore elute after larger biomolecules. The wells were equilibrated according to the manufacturer's instructions using 300 µl of storage buffer. The eluted fractions from the protein purification were added (entire 160 µl) and were incubated for 3 min at room temperature with the resin in the well. The plate was then centrifuged at 800 xg for 2 min at 4 °C to collect the protein.

Test set

Test set variants were purified in a batch mode purification protocol using Ni-NTA agarose (Qiagen) and were desalted by gravity flow using a MiniTrap G-10 desalting column (Cytiva) followed by concentrating the sample using a 10 kDa molecular weight cutoff centrifugal spin filter (Merck).

A total of 400 µl Ni-NTA agarose was washed by resuspension in 4000 µl of wash buffer and then centrifuged at 900 xg for 3 min followed by discarding the supernatant. This was repeated 3 times. After that, 600 µl lysed cell solution treated as previously described was added to the agarose and incubated on ice for 1 hour on a shaking bed. Incubated samples were then centrifuged at 900 xg for 5 min followed by discarding the supernatant containing any unbound proteins from the cell lysate. The agarose containing bound protein was then washed 3 times using 2000 µl wash buffer followed by centrifugation at 900 xg for 5 min. As a final step, the agarose was resuspended in 110 µl of elution buffer and let incubate for 1 min on ice followed by centrifugation at 900 xg for 3 min to collect the eluted cy-F/SBPase protein. This step was repeated for a total of 5 times to ensure that most of the protein got eluted from the agarose.

Eluted protein fractions were then buffer exchanged into storage buffer using a PD-10 desalting column. The desalting columns were equilibrated using storage buffer according to the manufacturer's instructions. Each collected elution fraction from the purification was added to the column and 1500 µl of storage buffer was used to elute the buffer exchanged protein sample from the column. Protein samples were then concentrated to a final volume of 75-100 µl using a 10 kDa molecular weight cutoff centrifugal spin filter (Merck).

4.6 Measuring protein concentration

The concentration of purified protein samples was determined using a commercial Bradford colorimetric assay (Bradford ULTRA, Abcam). The assay applies Coomassie Brilliant Blue dye which complexes with the protein sample resulting in an absorption maximum at 595 nm (Wilson & Walker, 2018). Protein samples were mixed together with the dye at a 1:15 volumetric ratio and measured at 595 nm on a SpectraMax i3x

microplate reader in a 96 clear well plates (Greiner). The protein concentration was determined with the help of a prepared standard curve over 10 dilutions of bovine serum albumin ranging between 0.025 and 1 mg/ml.

4.7 Enzyme assay

The enzymatic activity of cy-F/SBPase variants was determined using a Malachite Green assay which is based on colorimetric detection of P_i ions in solution. The assay was adapted from Vardakou et al. (2014) and performed in clear 96 well flat bottom plates (Greiner) according to the workflow in Figure 11. A full overview of the preparation of all reactants and how they were used when assaying the validation and test set mutants is given in Table A2.

Each well was loaded with 100 µL of dilution buffer (50 mM Tris-HCl pH 8, 15 mM $MgCl_2$) and 36 µL of development solution (1.6 g/L malachite green oxalate salt in 3M sulfuric acid, 7.5 g/l ammonium molybdate·$4H_2O$ and aqueous 11% Tween20 which was filtered through a 0.2 µm filter to remove precipitates). The ratio of MG oxalate solution to ammonium molybdate solution in the development solution was varied in a set of optimization experiments which is discussed in section 7.2, whereas the volume of Tween20 was kept the same for all experiments.

The enzymatic reaction was performed in PCR tubes in a thermocycler set to 30 °C. The enzyme (1.8 µg/ml) was pre-incubated in reaction buffer (50 mM Tris-HCl pH 8, 15 mM MgCl2) containing varying concentrations of DTT (as discussed in Results section 5.3.1) in 90% of the final reaction volume at 30 °C for 10 min. Subsequently, different substrate stock solutions in the range of 100-5000 µM were added to 10% of the final reaction volume. End-point measurements were performed by running the reactions for 20 min whereupon 20 µl of the enzymatic reactions were quenched by transferring to the development plate. A P_i standard curve using $Na_2HPO_4·2H_2O$ in reaction buffer was included on each 96-well plate in the range of 0-100 µM. The plate was then covered in aluminum foil and incubated for 20 min at room temperature to allow complete color development. Absorbance was then measured at 620 nm on the Spectramax i3x photometer.

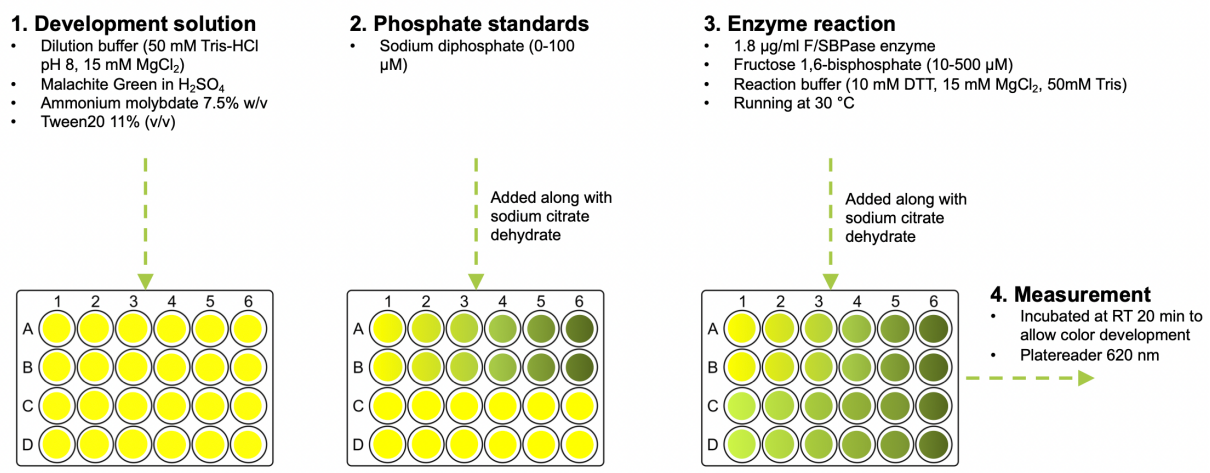

Figure 11 – The workflow for the applied kinetic assay.

The concentration of P_i was then quantified in relation to the standard curve. Initial experiments confirmed the linearity of substrate accumulation over time in between 0 and 20 min for all substrate concentrations used so that endpoint measurements at 20 min were used as a surrogate for sampling at several time points. The resulting initial rates were plotted over substrate concentration and fitted to the Hill equation (Equation 3) to determine the kinetic parameters k_{cat}, K_M and the hill coefficient n using the solver function in Microsoft Excel.

5. Results

5.1 Preparation of expression vectors carrying cy-F/SBPase variants

Before studying the enzymatic activity of the different cy-F/SBPase variants *in vitro* the respective gene fragments were cloned into an expression vector. In a first step the commercially obtained gene fragments were amplified by PCR. Subsequently both the pET28a(+) vector and the inserts were digested with *XhoI* and *NdeI* restriction enzymes (Figure 12) followed by ligation as described in the Methods section 4.3.

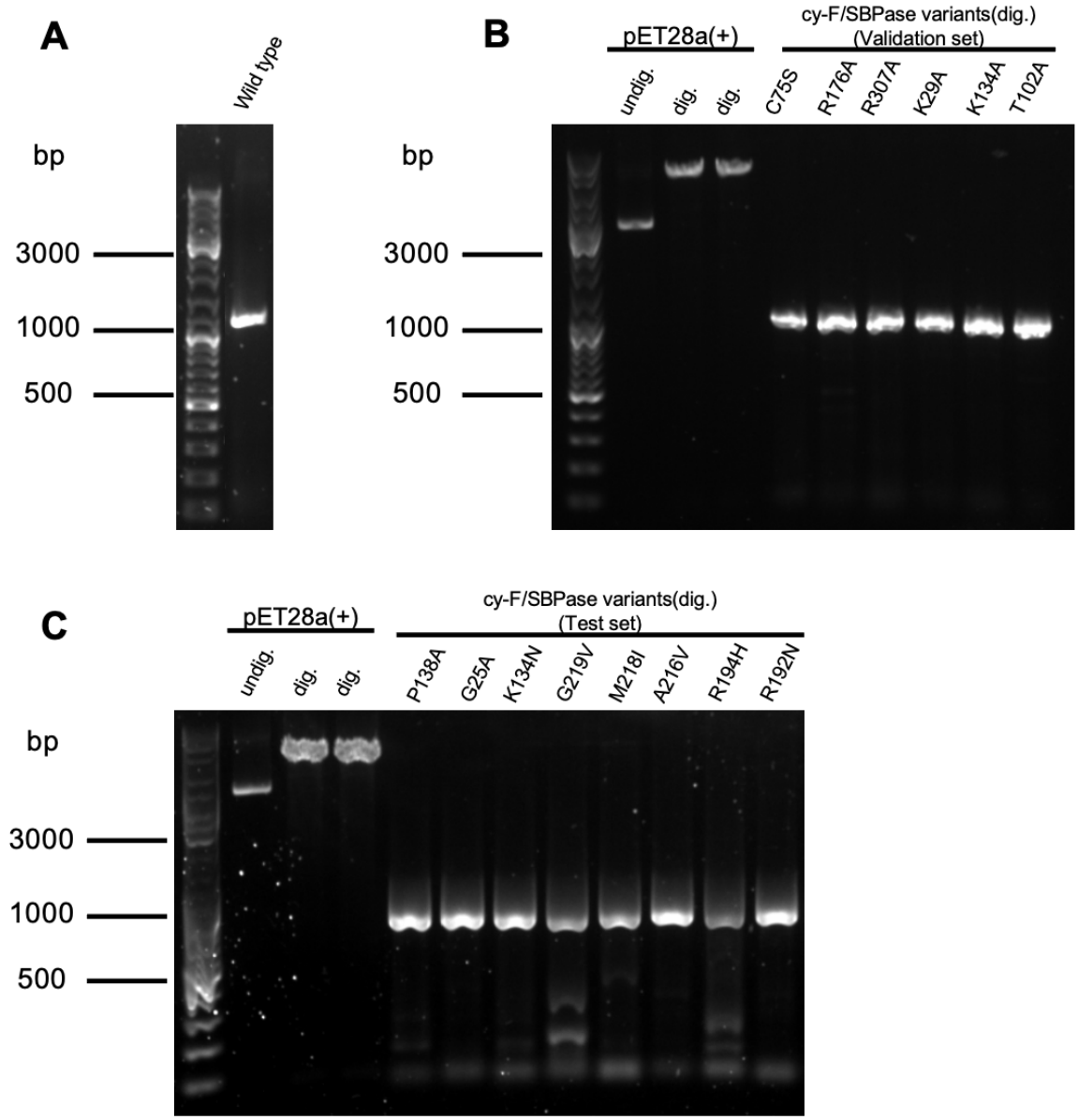

Figure 12 – A) Digested wild-type insert. B) Undigested and digested pET28a(+) vector as well as digested variant inserts of the validation set. c) Undigested and digested pET28a(+) vector as well as digested variant inserts of the test set. C) Digested wild-type insert. The DNA ladder used is GeneRuler DNA ladder mix (ThermoFisher Scientific)..

The correct insertion and sequence of all variants was confirmed by sequencing with exception of T102A that had an additional point mutation at residue position 127 where an alanine was mutated to a cysteine.

5.2 Expression and purification of cy-F/SBPase variant enzymes

5.2.1 Wild type and validation set variants

The validation and test set variants along with the wild type were expressed in *E. coli* and purified using immobilized nickel ion chromatography as described in detail in the Methods sections 4.4 and 4.5. Soluble fraction of bacterial lysates and the first two elution fractions for the wild type and validation set variants can be seen in Figure 13.

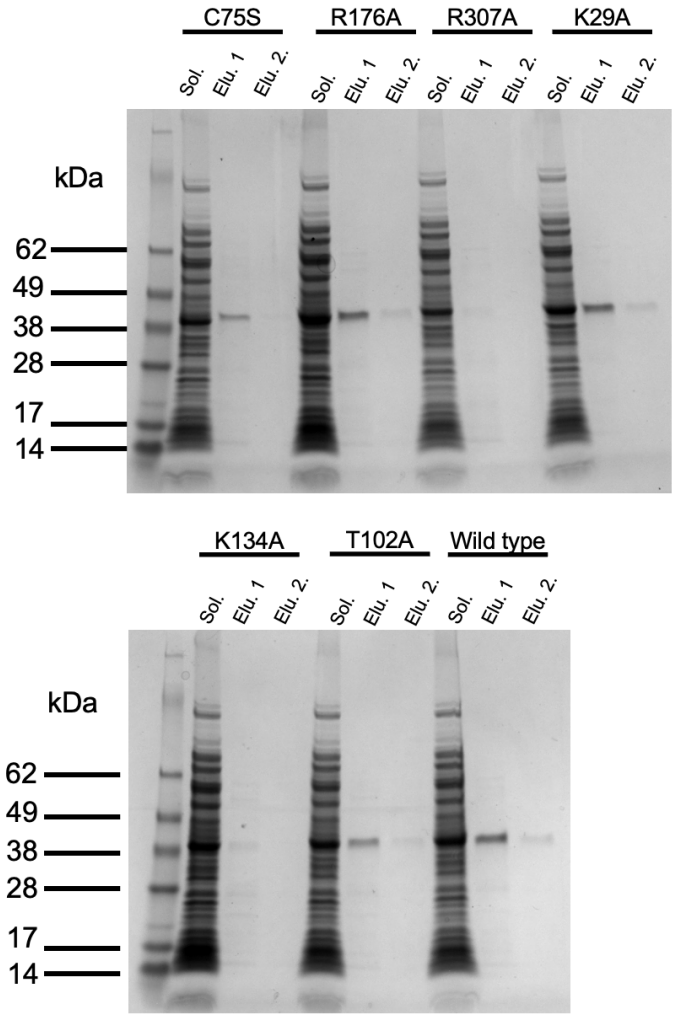

Figure 13 – Soluble fractions of bacterial lysate (Sol) as well as elution fractions (Elu) 1 and 2 for cy-F/SBPase variants of the validation set and wild type. The protein ladder used is SeeBlue Plus2 Pre-stained Protein Standard (Bio-Rad).

The R307A and K134A variants of cy-F/SBPase in the elution fractions were not present in the elution fractions at an adequate concentration and as a consequence were not assayed.

5.2.2 Test set variants

The variants in the test set were purified using a batch purification protocol since plate-format purification (as shown in Figure 13) resulted in low protein yields with concentrations at the lower detection limit of the employed Bradford assay. The elution fractions for the test set mutants purified with this protocol can be seen in Figure 14.

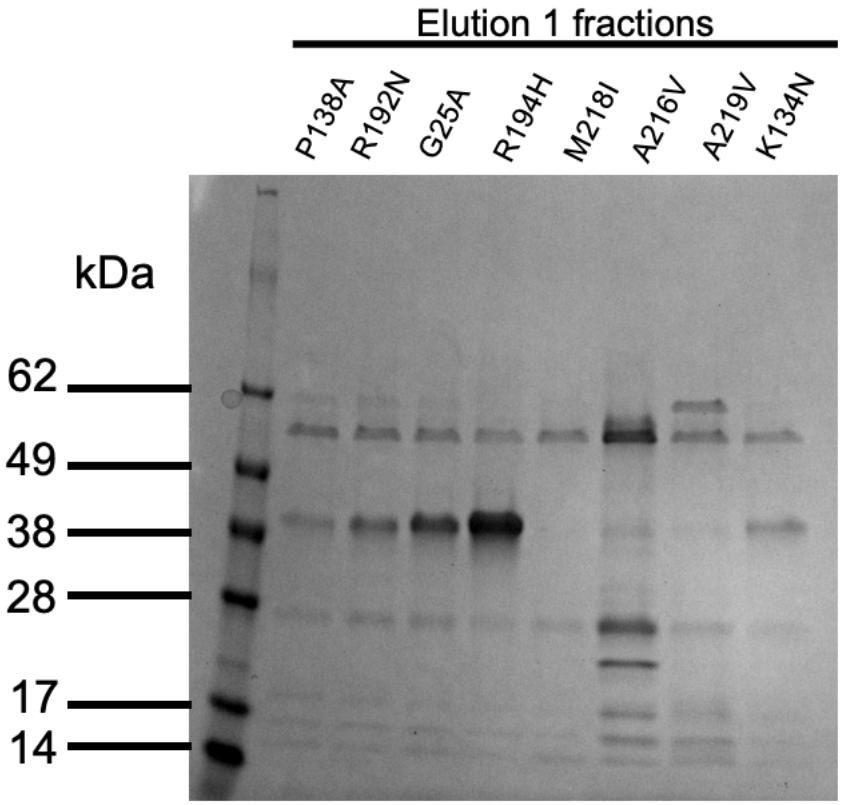

Figure 14 – Elution 1 fractions for cy-F/SBPase variants of the test set. The protein ladder used is SeeBlue Plus2 Pre-stained Protein Standard (Bio-Rad).

5.3 Malachite green enzyme activity assay of cy-F/SBPase variants

5.3.1 Assay optimization

Before measuring the kinetic parameters of the purified cy-F/SBPase variants with the Malachite Green assay, the assay protocol for colorimetric detection was optimized for

the specific buffer conditions of the enzymatic reaction in order to obtain a maximal signal-to-noise ratio.

Malachite green to molybdate ratio

In order to evaluate if the ratio of malachite green (MG) to ammonium molybdate in the development solution can influence the degree of color separation between different Pi concentrations in the sample solution, a titration experiment was performed. In a first step, the volumes of MG dye stock (1.6 g/L malachite green oxalate salt in 3 M sulfuric acid) and 7.5 g/l ammonium molybdate·$4H_2O$ solution were therefore varied with respect to each other in 10 different combinations. A 20 µl sample consisting of wild-type cy-F/SBPase (1.8 µg/ml) that had been incubated with 500 µM FBP in reaction buffer for 20 min at 30 °C was added to 36 µl of each the 10 different development solutions and 100 µl dilution buffer (50 mM Tris-HCl pH 8, 50 mM $MgCl_2$). A volume of 20 µl of P_i containing 1 µM, 10 µM, and 50 µM disodium phosphate standard in reaction buffer were also incubated with the different development solutions. A sample consisting of only reaction buffer (50 mM Tris-HCl pH 8, 15 mM $MgCl_2$, 10 mM DTT) representing the blank sample was also added to each of the 10 development solutions. All samples were loaded onto the same 96-well plate which was then visually inspected to identify the conditions for the clearest color separation between the different P_i standard concentrations and to confirm that the color from the enzyme reaction was within the range of the P_i standards. The results are shown in Figure 15.

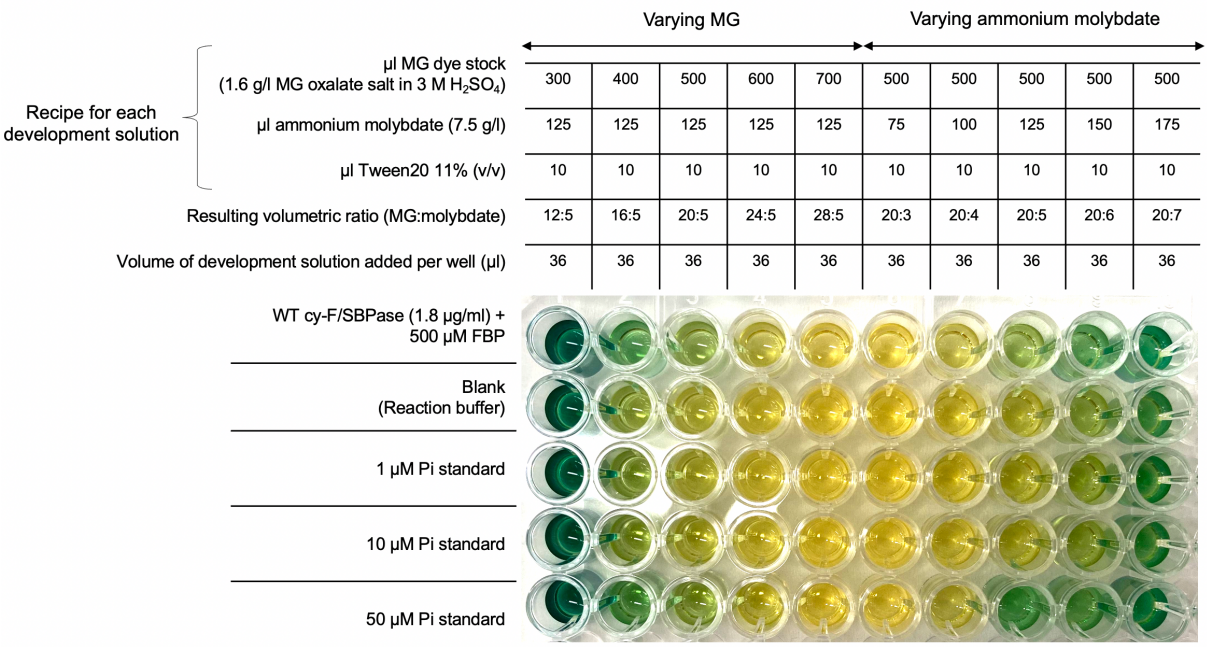

Figure 15 – Malachite green (MG) colorimetric detection of cy-F/SBPase reaction product and different P_i standards along with blank sample containing only reaction buffer. Ten different versions of the development solution were prepared in which the volume of MG dye stock to ammonium molybdate solution was varied as indicated. The concentration of all development solution components that were added together in different ratios can be seen to the left.

DTT concentration in the reaction buffer

DTT is used in the enzyme reaction buffer to ensure that the enzyme is in its active state (as described in section 3.1). To determine its optimal concentration in the reaction mix (i.e. yielding high activity at low background color levels) three wild-type cy-F/SBPase reactions (1.8 µg/ml) with 500 µM FBP were prepared with 10 mM, 15 mM and 20 mM DTT in the reaction buffer, respectively. The reactions were incubated at 30 °C for 20 min whereupon each 20 µl of the reactions were added to 100 µl dilution buffer and 36 µl development solution in the same 96 well plate. The results were analyzed with respect to the DTT concentration that yielded clearest color separation (Figure 16).

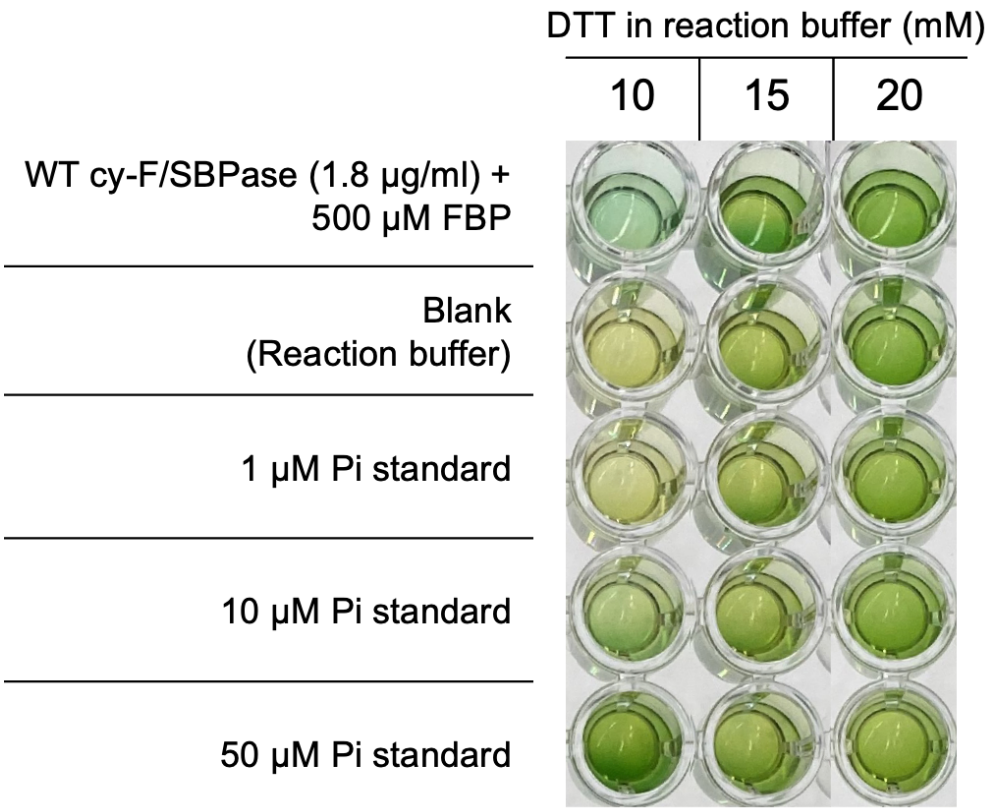

Figure 16 – Malachite green colorimetric detection of cy-F/SBPase reaction product and different P_i standards using three different concentrations of DTT in the reaction buffer.

Effect of citrate on color stability

A previous study applying the malachite green assay mentions the possibility of nonenzymic hydrolysis of substrate which can generate P_i that causes color fluctuations and inaccurate absorbance measurements (Rowlands et al., 2004). Another study discovered that the addition of 34% w/v sodium citrate after sampling the reaction resulted in less undesired post-quenching color development (Lanzetta et al., 1979). This was investigated to see if color stability when assaying cy-F/SBPase could improve by the addition of sodium citrate.

In order to test the effect of sodium citrate on unspecific color development after quenching the enzymatic reaction, four replicates of cy-F/SBPase reactions and P_i standards were prepared according to the protocol mentioned in section 4.7. Right after quenching the reaction by adding 20 µl of each reaction to the development solution, 7.5 µl of 34 % (w/v) sodium citrate dihydrate in filtered dH_2O water was added to the wells for two of the four reactions (2 replicates for added citrate and 2 controls

without citrate) and the solution in the well was mixed thoroughly by pipetting up and down. Absorbance of the samples in the 96-well plate was then measured in a plate reader every 5 min for a total of 1 hour. The absorbance of the sampled enzyme reactions and P_i standards with and without addition of citrate after quenching was then plotted for the various timepoints (shown in Figure 17 for enzymatic reactions and Figure 18 for the P_i standards). A linear regression of the data points was performed to highlight the trend of the change in absorbance over time.

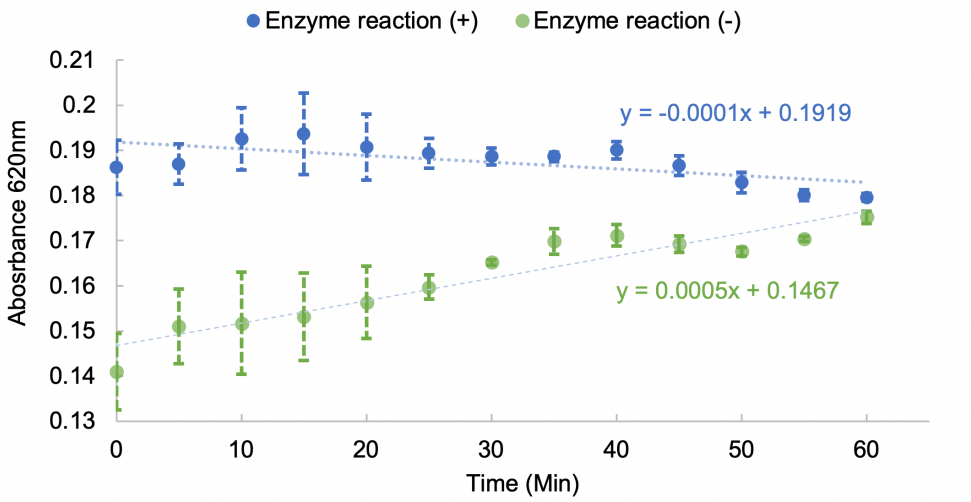

Figure 17 – Absorbance plotted over time for sampled cy-F/SBPase reaction with 500 µM FBP with (+) and without (-) citrate added to the development solution after quenching. The equations show the linear regression for their corresponding data points in the same color. Colored error bars represent the standard deviation for duplicate measurements.

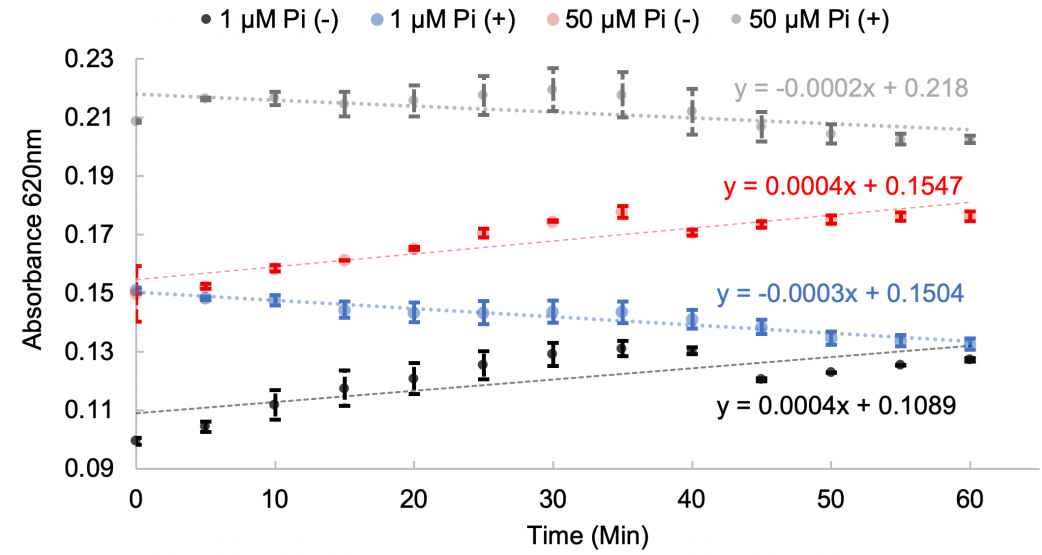

Figure 18 - Absorbance over time for the P_i standards with (+) and without (-) citrate added to the development solution after quenching. The equations show the linear regression for their corresponding data points in the same color. Colored error bars represent the standard deviation for duplicate measurements.

5.3.2 Activity of cy-F/SBPase variants

The optimized assay conditions as described in 6.3 were used to study the activity of wild-type and variant cy-F/SBPases (validation and test sets). Cy-F/SBPase enzymes were incubated in reaction buffer (50 mM Tris-HCl pH 8, 15 mM $MgCl_2$, 10 mM DTT) with substrate concentrations ranging from 10-500 µM for a total time of 20 min. Reactions were quenched by transferal to 100 µl dilution buffer and 36µl development solution (400 µl 1.6 g/L malachite green oxalate salt in 3M sulfuric acid, 125 µl 7.5 g/l ammonium molybdate·$4H_2O$ and 10 µl of aqueous 11% Tween20 which was filtered through a 0.2 µm filter) and addition of 7.5 µl 34 % (w/v) citrate as color stabilizer. P_i accumulation over time was quantified in relation to a standard curve (2.2 – 100 µM, R^2 values ranging from 0.950 to 0.993) on the same plate. Initial rates v_0 were determined as the slope of product accumulation over time within the linear range of the standard curve. Normalized initial reaction rates ($v_0/[E]$) for each variant were then plotted over corresponding FBP concentrations and fitted to the Hill equation (Equation 3) using non-linear least square regression as shown in Figure 19, 20 and 21. The kinetic constants of the Hill equation for each cy-F/SBPase variant can be found in Table 1.

Table 1

The kinetic constants K_M, k_{cat}, k_{cat}/K_M and hill coefficient *n* for the WT cy-F/SBPase and the assayed mutants. The data from the wild-type variant (WT) is averaged duplicates from three different occasions it was assayed whilst the data for the remaining variants is from duplicates of one assay occasion.

Cy-F/SBPase variant	K_M (µM)	k_{cat} (s^{-1})	k_{cat}/K_M ($M^{-1}s^{-1}$)	*n*
Validation set				
WT	85.1 ± 6.13	6.26 ± 1.59	(7.40 ± 1.32) × 10^4	1.83 ± 0.23
WT*	80.0 ± 10.0	10.5 ± 0.500	1.30 × 10^5	1.90 ± 0.40
WT (-) DTT	16.3 ± 9.51	1.60 ± 0.345	(9.8 ± 2.6) × 10^4	1.09 ± 0.61
WT (-) DTT*	N.D	3.00	N.D	N.D
K29A	171 ± 39.1	23.0 ± 4.74	(1.34 ± 0.03) × 10^5	2.59 ± 0.330
K29A*	150 ± 20	21.3 ± 1.00	1.40 × 10^5	2.00 ± 0.400
C75S	94.4 ± 13.7	6.46 ± 0.169	(6.83 ± 0.730) × 10^4	2.17 ± 0.310
C75S*	N.D	14.0	N.D	N.D
C75S (-) DTT	94.2 ± 5.04	6.02 ± 0.367	(6.40 ± 0.052) × 10^4	2.13 ± 0.160
C75S (-) DTT*	N.D	15.0	N.D	N.D
R176A	N.D	N.D	N.D	N.D
R176A*	3200 ± 300	0.700 ± 0.030	2.1 × 10^2	1.20 ± 0.100
Test set				
G25A	128 ± 50.6	0.916 ± 0.021	(7.17 ± 2.72) × 10^3	0.410 ± 0.018
K134N	6.32 ± 0.115	0.339 ± 0.011	(5.35 ± 0.087) × 10^4	1.90 ± 0.356
P138A	N.D	N.D	(3.00 ± 0.014) × 10^2	N.D
R192N	285 ± 2.51	1.87 ± 0.159	(6.55 ± 0.675) × 10^3	0.518 ± 0.004
R194H	1400 ± 86.3	3.18 ± 0.197	(2.27 ± 0.019) × 10^3	0.472 ± 0.006
A216V	31.6 ± 13.3	0.510 ± 0.049	(1.61 ± 0.353) × 10^4	0.846 ± 0.298
G219V	N.D	N.D	(0.90 ± 0.37) × 10^2	N.D

* Kinetic data from Feng et al (2014)

DTT, Dithiothreitol addition

N.D, Not determined.

Validation set

To evaluate the accuracy of the colorimetric assay a series of previously kinetically characterized cy-F/SBPase variants (described in section 3.4) was studied. Among these, R307A, K134A and T102A were not assayed since they either showed an unspecific mutation in the sequence or were not obtained in sufficient yield.

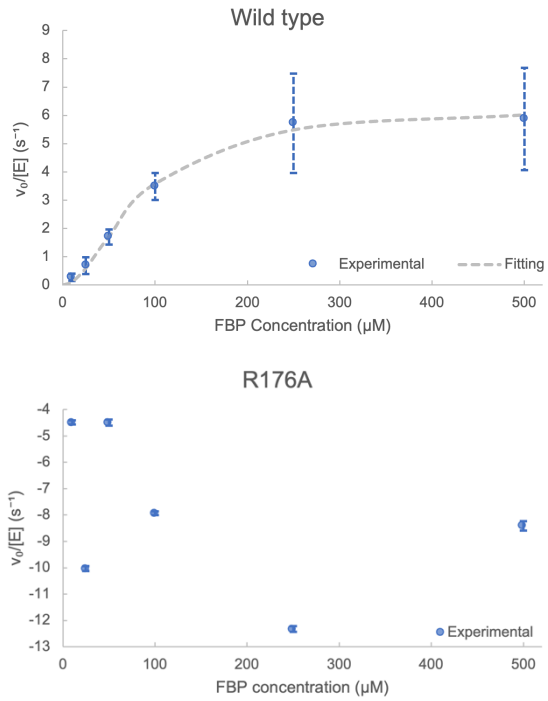

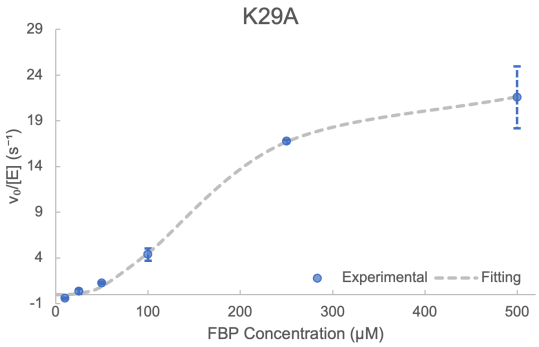

Figure 19 – Michaelis Menten plots for the assayed variants of the validation set. Normalized initial reaction rates $v_o/[E]$ (blue dots) were plotted over respective substrate concentration of fructose 1,6-bisphosphate (FBP) and fitted to Equation 3 (grey dashed line). Error bars colored blue represent the standard deviation from six replicates for the wild type and duplicates for the K29A and R176A variants.

Cy-F/SBPase C75S activity measurement in absence of DTT

Another set of experiments aimed at reproducing the described dependency of cy-F/SBPase wild-type activity on DTT in the reaction buffer as well as the elimination of this dependency in the C75S variant as published by Feng et al (2014). The results are shown in Figure 20 and summarized in Table 1.

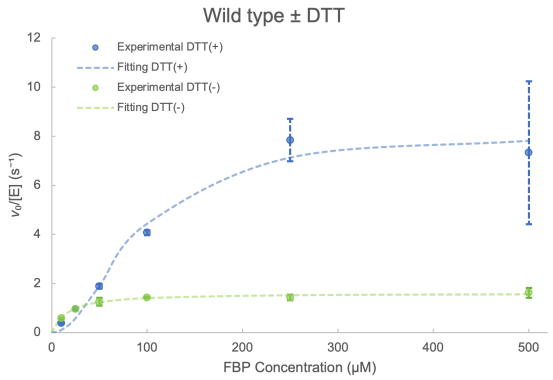

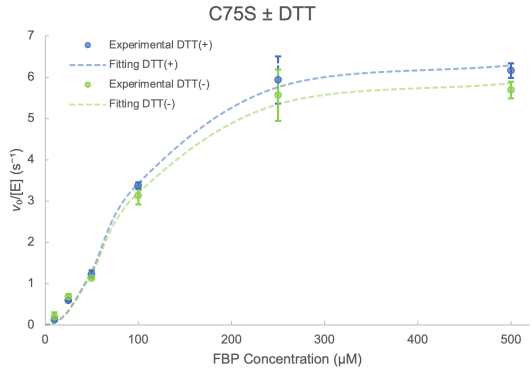

Figure 20 – Michaelis Menten plots for the wild type and C75S variant of the validation set. Normalized initial reaction rates $v_o/[E]$ for with (blue dots) or without (green dots) 10 mM DTT in the reaction buffer were plotted over their respective substrate concentration of fructose 1,6-bisphosphate (FBP). The measured reaction rates were fitted to Equation 3 using non-linear regression (colored dashed line). Colored error bars represent the standard deviation for duplicate measurements.

Test set

The goal of assaying the test set mutants was to obtain an initial understanding of how certain residue exchanges between the active site and allosteric site affect enzyme activity. All test set mutants were assayed simultaneously in duplicates using end-point measurements.

Since the G219V and P138A variants of cy-F/SBPase did not reach substrate saturation, catalytic efficiency was quantified using the slope from a linear regression. One datapoint each from P138A and G219V was omitted to obtain a better fit (orange dots in Figure 21). Variant M218I was not assayed due to being absent in the elution fraction during purification as seen in Figure 14. Figures 22 and 23 visualize the data in Table 1 to compare the relative difference of K_M, k_{cat} and k_{cat}/K_M between the wild type and test set variants when assayed together.

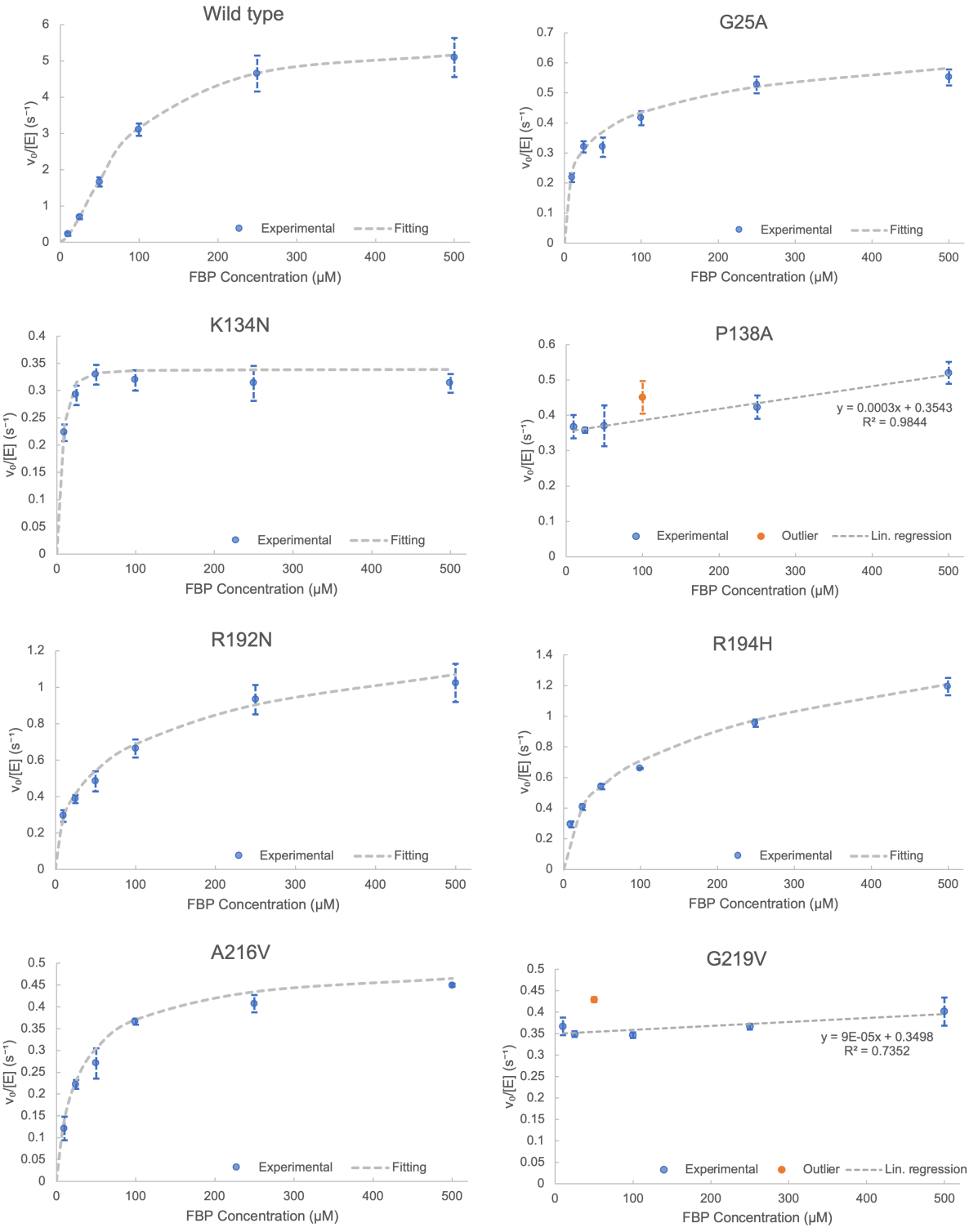

Figure 21 – Michaelis Menten plots for the assayed variants of the test set. Normalized initial reaction rates vo /[E] (blue dots) were plotted over respective concentrations of fructose 1,6-bisphosphate (FBP) and fitted to Equation 3 using non-linear regression (grey dashed line) or by linear regression (blue dashed line). Error bars colored blue represent the standard deviation for duplicate measurements.

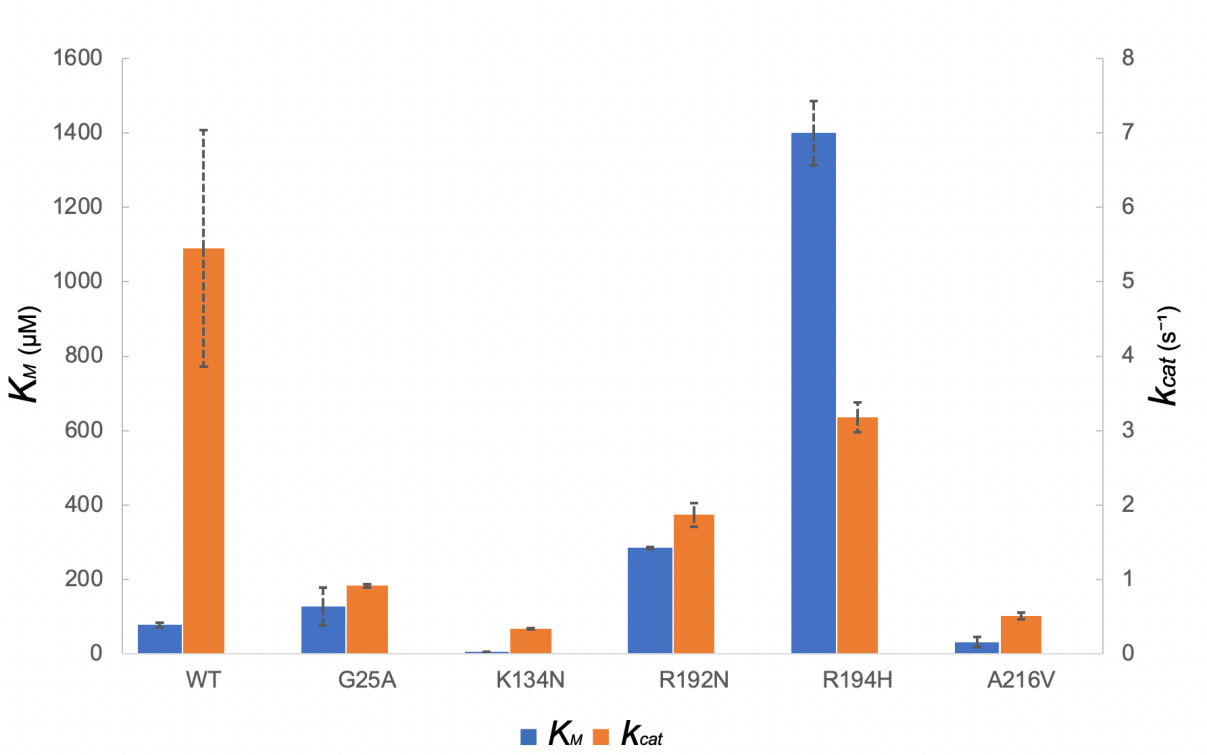

Figure 22 – Obtained Michaelis constants (K_M) and turnover numbers (k_{cat}) of cy-F/SBPase variants from the test set. Error bars in black represent the standard deviation for duplicate measurements.

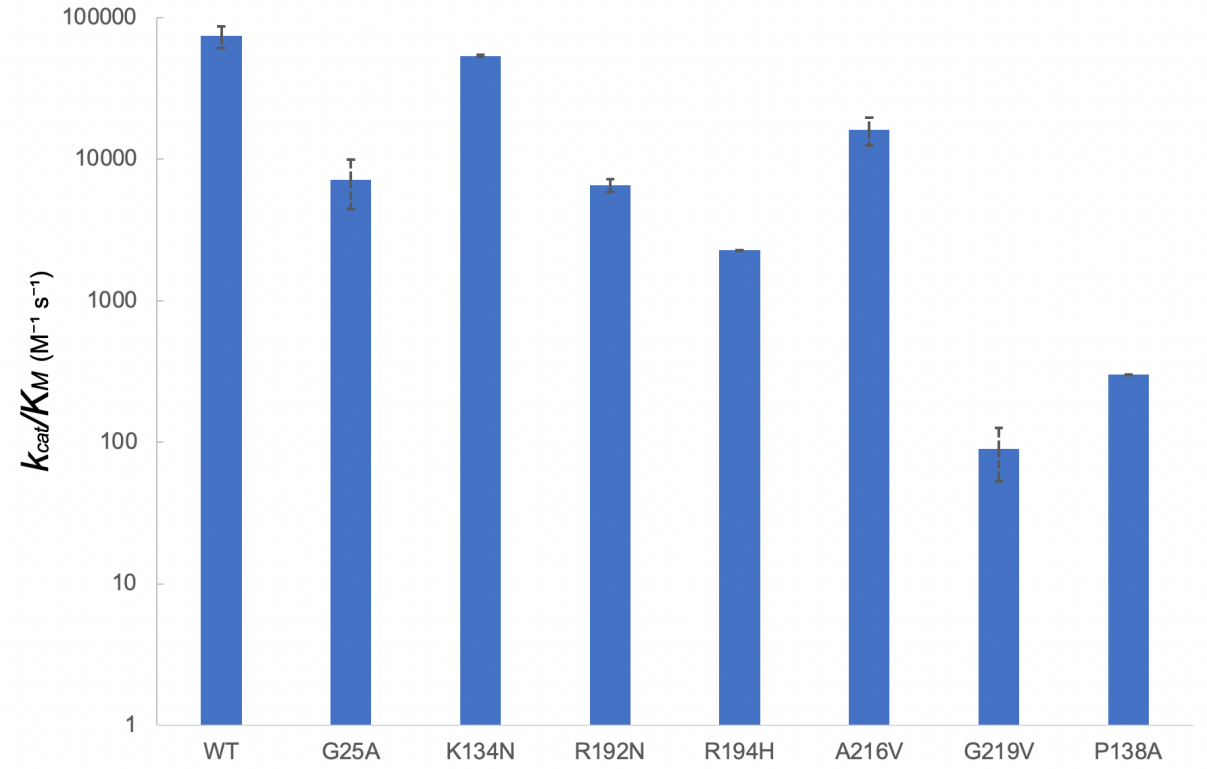

Figure 23 – Kinetic efficiency k_{cat}/K_M of cy-F/SBPase variants from the test set. Error bars in black represent the standard deviation for duplicate measurements.

6. Discussion

6.1 Cloning, expression and purification

Wild-type cy-F/SBPase as well as the validation and test set gene inserts were successfully cloned into the pET28a(+) vector as judged from the sequencing data. However, variant T102A and K134A showed unspecific mutations in the insert sequence. Variant T102A showed an additional mutation at residue position 127 where alanine was mutated to cysteine. Alanine is a small and flexible residue that does not form side-chain hydrogen bonds (Berg et al., 2015). An alanine to cysteine exchange could potentially lead to the formation of additional disulfide bonds with other cysteine residues in the same or in other protein monomers. Since residue 127 is located on the surface of the cy-F/SBPase subunit there is a probability that such a disulfide bond could result in incorrect subunit assembly and in turn generate an inactive enzyme. Consequently, this variant was not assayed. Variant K134A was not assayed either due to a detected base pair deletion at position 42. Moreover, R307A was also not assayed due to poor protein yield upon purification in relationship to the other variants on the SDS-PAGE gel (See Figure 13). It can be ruled out that they did not express as soluble form since a strong band of correct size is visible in the soluble fraction of the bacterial lysates. One possible explanation is that these proteins were lost during purification by not properly binding to the Ni^{2+} agarose resin in the His MultiTrap FF plate. As a consequence, the protein may have eluted already in the flow through or wash fractions. Due to the lack of time, it was not possible to express and purify K134A and R307A again. If this experiment was to be repeated one might try using a lower imidazole concentration in the lysis and wash buffers to prevent loss of protein due to insufficient binding.

For the purification of the test set variants, a batch purification was used because the plate-based purification yielded low protein concentrations (0.05 – 0.182 µg protein/ml cell culture). At the same time, the desalting plate elution volume (100 µl) was too small to concentrate the protein variants using centrifugal spin filters. Compared to the plate-based purification the batch protocol allows custom volumes of wash- and elution buffer, as well as prolonged incubation of bacterial lysates with the resin, therefore potentially allowing more efficient protein recovery. Despite an overall increased protein yield (0.17-0.64 µg protein/ml cell culture), the purity of these variants was

deteriorated compared to the plate-based protocol as seen in Figure 14, where several additional bands are clearly observed. Nevertheless, the cy-F/SBPase band on the SDS-PAGE gel was visible in reasonable purity compared to the total bacterial lysate from a different gel, which is why the enzyme variants were assayed, nonetheless. Since the actual cy-F/SBPase concentration in the desalted purified sample was lower than the total protein concentration measured in the Bradford assay, an image processing software (ImageJ) was used to quantify the band intensity for cy-F/SBPase at 38 kDa and the sum of intensities for all bands in the respective lane. The cy-F/SBPase band intensity was divided by the total band intensity to acquire the ratio of cy-F/SBPase to other proteins in the sample. Acquired ratios were between 0.2-0.6 for all different variants. The acquired protein concentration from the Bradford assay was then multiplied by this ratio to estimate the actual concentration of the cy-F/SBPase variants.

6.2 Colorimetric assay optimization for cy-F/SBPase

The Malachite Green assay is an established assay for quantifying P_i in solutions and has been previously used to assay activity of enzymes that release P_i as part of their substrate conversion (Geladopoulos et al., 1991; Zhou & Arthur, 1992). Since a commercial Malachite Green assay kit appears to be used in the reference study whereas a “self-made” assay (based on a protocol by Vardakou et al.) was employed in this study, a few optimizations of the parameters of colorimetric detection were performed in order to ensure an optimal signal-to-noise ratio.

Development solution

Besides quenching the enzymatic reaction due to its low pH, the development solution contains molybdate ions that form a complex with P_i in solution as well as MG salt that then forms a green complex with the molybdate-P_i complex, as described in Background section 3.3.

Since the optimal relative amount of molybdate to MG can vary with the reaction buffer used in the experiment, a titration experiment was performed in which a series of development solutions with varying volume proportions of MG and molybdate was prepared and tested both with the Pi standards and a cy-F/SBPase reaction. Based on

what is presented in Figure 15 it can be seen in columns corresponding to volume ratios of 24:5, 28:5, 20:3 and 20:4 (MG dye stock solution : ammonium molybdate solution) there is no color development at all. This could signify that the amount of excess MG dilutes the sample enough to the point of no green color being visible. For columns in which the ratio was 12:5 and 20:7 a strong colorimetric signal was observed in all wells but no difference in colorimetric intensity was distinguishable for samples with different concentrations of Pi. When using ratios of 16:5, 20:5 and 20:6 in the development solution a clear colorimetric signal for the 50 µM P_i standard and cy-F/SBPase reaction product could be seen. Among these, the difference in color intensity between the 50 µM Pi standard to Pi standards of lower concentration (1 µM and 10 µM) was most distinct for the ratio of 16:5. It also gave a clearer color difference between the blank and the 1 µM and 10 µM Pi sample while ratio 20:5 did not. The recipe of this development solution was therefore used in all subsequent MG assays. Moreover, using this development solution led to the greatest color separation between the Pi standards and the blank whilst the color of the cy-F/SBPase reaction product was within the range of the Pi standards. It is noteworthy that the blank samples for ratios 12:5, 16:5, 20:5, 20:6 and 20:7 in which no Pi is present demonstrate a certain degree of color development. The reason for this is unclear. One explanation could be that a green MG-molybdate complex could be formed when molybdate is in excess.

The effect of DTT concentration on color development

DTT is added to the cy-F/SBPase reaction as reducing agent to ensure that the enzyme is in its reactive state in which the disulfide bridge between C75 and C99 is not formed (Feng et al, 2014). Since it is a heat sensitive compound (Pubchem, 2021) DTT likely gets degraded over time in the enzymatic reaction which runs at 30°C. Hence, it might be desirable to use a higher concentration than that mentioned in the paper by Feng et al (2014) to compensate for the degradation of DTT. One potential pitfall of using a higher DTT concentration is that it may increase the background signal and give an inseparable color between samples with varying degree of P_i concentration. The concentration of DTT in the reaction buffer was therefore varied and the colorimetric signal of cy-F/SBPase reaction product, blank as well as different P_i standards that were diluted in the same reaction buffer was measured. In Figure 16, a DTT concentration of 15 or 20 mM in the reaction buffer gave rise to an almost

indistinguishable color difference between the blank and Pi standards. In contract, using 10 mM DTT in the reaction buffer resulted in a color signal for the enzymatic reaction that was within the range of the Pi standards. Moreover, the color signal increased roughly proportionally with the concentration of Pi in the different standards. The increase in green color intensity at higher DTT concentrations may result from molybdenum redox species in the development solution caused by the reducing properties of DTT. Molybdenum which exists as MnO_4^{-2} in the development solution has an oxidation number of +6 which makes it susceptible to being reduced. These redox species could potentially react with the MG dye in a similar fashion to the molybdate-Pi complex and result in color development.

Effect of citrate on color stability

When using the assay conditions as previously described, a considerable increase in colorimetric signal after quenching was observed over time (Figure 17 and 18). The fact that the slopes of increase in colorimetric signal were similar for different P_i standards (Figure 18, black and red graphs) as well as the cy-F/SBPase reaction product (Figure 17, green graph) suggests that this increase is not due to incomplete quenching of the reaction but rather represents a general unspecific color development. As described in section 6.3.1 citrate is commonly added to the MG development solution as a color stabilizer after quenching. In line with these protocols, the addition of citrate to the development solution after quenching had a positive effect on color stability over time. Using citrate in the development solution for the enzyme reactions resulted in a decrease in the steepness of the slopes for both enzymatic reaction and P_i standards (Figure 17 and 18). Consequently, citrate was added post-quenching in all subsequent MG assays.

6.3 Activity of cy-F/SBPase variants

A series of cy-F/SBPase variants was assayed using the presented MG colorimetric assay. The accuracy of the assay in capturing a range of phenotypic effects conferred by different single residue exchanges was assessed using a test set of variants that have been previously fully kinetically characterized. A set of 8 single residue exchange variants that have not been kinetically characterized before were studied in a similar manner to see how certain point-mutations impact activity.

Validation set

Wild-type cy-F/SBPase and variants K29A, C75S, T102A, K134A, R176A, R307A were included in the validation set. The results as seen in Table 1 for wild-type cy-F/SBPase, K29A and C75S displayed very similar K_M and Hill coefficients to the parameters obtained from the reference paper by Feng et al (2014. This shows that the substrate affinity and cooperative effect of cy-F/SBPase were accurately described with the assay presented in this thesis. In contrast, the turnover number k_{cat} was 40% lower than reported in the reference paper. In theory k_{cat} is a constant but differences in experimental conditions such as pH and temperature can affect this parameter. For example, the pH-value can alter the protonation states of key amino acids involved in catalysis (Wilson & Walker, 2018). The temperature of the reaction also has an impact on the activation energy for the catalytic reaction (Berg et al., 2015). Since the thermocycler was opened during the assay when different time points were sampled from the enzymatic reaction, there could have been a temporary decrease in temperature which may explain the observed differences in k_{cat} values between this thesis and the reference study. Similar to wild-type cy-F/SBPase, the kinetic parameters for variant K29A as seen on Table 1 were within the same order of magnitude as those in the reference paper.

In contrast, no reliable kinetic data could be obtained for the R176A variant (Figure 19). It is known that this residue exchange results in a reduction of k_{cat} from 10.5 s^{-1} to 0.7 s^{-1} which is among the lowest turnover numbers presented among all variants in Feng et al (2014). It is likely that the colorimetric assay in this thesis is therefore not sensitive enough to detect this activity. Another possible explanation may be that the purified enzyme was completely inactive. In the reference paper, k_{cat} for the wild type was almost 15 times higher than that of the R176A. This would imply that at substrate saturation and constant enzyme concentration it would take variant R176A approximately 15 times longer to generate the same amount of P_i in comparison to the wild type unless the enzyme concentration for R176A is increased to match the activity of the wild type. If insufficient amounts of P_i (i.e. less than the sensitivity threshold of the assay) are generated from the enzyme reaction, there would not be any measurable increase in P_i over time. This could have happened when assaying R176A

since negative Pi concentration values were obtained due to absorbance readings outside of the Pi standard concentration range.

Finally, the C75S variant of cy-F/SBPase was studied and compared to the wild type. DTT was added to the reaction buffer as it is required to maintain cy-F/SBPase in an active conformation. This is due to the fact that the tense state conformation of F/SBPase is likely stabilized by a disulfide bridge between C75 and C99 which gets disrupted by the reducing agent (Feng et al., 2014). This result was successfully reproduced as illustrated by the results in Figure 20 that show a drastic decrease in wild-type rate of P_i release when DTT was excluded from the reaction buffer. In comparison, C75S maintained its conversion rate both in the presence and absence of DTT as reported by Feng et al (2014).

Test set

After demonstrating that the assay that was developed in this thesis was able to reproduce several kinetic aspects that have previously been published, eight single residue exchange variants of cy-F/SBPase were characterized with the same assay in order to study the effect of changing residues in proximity to the active or allosteric site on enzyme activity. All variants could be successfully expressed and purified except for M218I as can be seen in Figure 14. One potential explanation for why it was not present in the elution fraction is that the M218I mutation could potentially disrupt the protein core packing, resulting in an unfolded protein that gets degraded by proteases in the host organism. When evaluating the kinetic parameters of these cy-F/SBPase variants, it needs to be taken into account that the enzyme solutions are not as pure (Figure 14) as the validation set variants (Figure 13), which may bias the results.

Two of the variants, P138A and G219V were not saturated within the substrate range used in this thesis, which is why the catalytic efficiency (k_{cat}/K_M) was obtained directly from the slope of their respective Michaelis Menten plots in Figure 21. It can be seen that there is an initial spike in $v_0/[E]$ (i.e. a non-negligible signal at the lowest substrate concentration used) followed by a slow increase in $v_0/[E]$ with increasing FBP concentration. One might assume that these variants have already reached substrate saturation at 10 µM FBP but it is unlikely that a point mutation distant from the active

site would have such a strong effect on K_M. An alternative hypothesis is that the initial high signal in $v_0/[E]$ stems from background signal in the assay setup. The k_{cat}/K_M value for P138A and G219V was 3.0×102 M^{-1} s^{-1} and 0.9×102 M^{-1} s^{-1}, respectively. Consequently, both of these variants exhibit a specificity constant that is more than 100-fold lower than that of the wild type. This could be indicative of impacts of the residue changes on both substrate binding and catalytic activity. The fact that the obtained soluble yields are very low as seen on Figure 14 for these two variants suggests that they may be entirely unfolded. It is also very likely that all of the measured variants suffer from background signal due to the impurities in the sample with P138A and G219V being the most prominent due to their low activity.

Next, the kinetic parameters k_{cat} and K_M were determined for cy-F/SBPase G25A, K134N, R192N, R194H and A216V were determined and compared to the wild type as shown in Figure 22. It is important to mention that the enzyme samples assayed were not as pure as those of the validation set. Hence, the reliability of the data should be understood as preliminary results that require further verification.

All of the test set variants seem to exhibit a lower k_{cat} in comparison to the wild type with the lowest being G25A, K134N and A216V. The glycine at position 25 is located at a subunit interface and the slight reduction in flexibility that occurs with exchanging this residue for alanine may therefore impact subunit assembly. This notion is supported by the change in cooperativity as is reflected by the drastic decrease of Hill coefficient (0.41) as compared to the wildtype (1.56). Even though the K_M value for this variant is slightly increased, the effect is less strong than the k_{cat} effect, indicating that substrate affinity may be less strongly impacted by this residue exchange. Residue R192 and R194 could potentially be of importance for substrate binding as both show an increase in K_M of 285 µM and 1400 µM in respect to that of the wild type (77.9 µM). This is an interesting observation since both of these residues are located close to the AMP binding site and could be indicative of that the AMP binding site has an influence on enzyme FBP hydrolysis even when AMP is absent. While K_M drastically increased for R194H, k_{cat} was relatively maintained in comparison to the other variants when comparing to the wild type. This could potentially indicate that residue R194 has a more important role in maintaining substrate affinity than substrate turnover. A general trend in Hill coefficient for all test set variants except K134N showed a much lower *n*-value

(between 0.410-0.850) in comparison to the wild type (1.56). An interesting follow-up experiment would be to measure AMP binding to see if these variants that show weaker cooperativity would be less sensitive to AMP.

7. Conclusion and outlook

In this thesis, a malachite green assay was optimized and used to kinetically characterize a set of bifunctional cy-F/SBPase variants for one of the substrates (fructose 1,6-bisphosphate). The accuracy of the assay was assessed by assaying a set of previously kinetically characterized cy-F/SBPases followed by testing the assay on a set of *de novo* designed cy-F/SBPases to get a crude understanding of how certain protein residue exchanges affect enzyme activity. An immediate next step would be to characterize the allosteric inhibition properties of G25A, K134N, R192N, R194H and A216V to see if the decrease in cooperativity translates to a lower sensitivity towards allosteric inhibition by AMP. It would also be interesting to express variant K29A that exhibited a double as high k_{cat} value to that of the wild type *in vivo* to see if this can have a positive effect on organismal growth rate and biomass yield.

8. References

Alon, U. (2007). *An Introduction to Systems Biology: Design Principles of Biological Circuits*. Taylor and Francis Group.

Amesz, J. (1987). *Photosynthesis* (Vol. 15). Elsevier Science LTD.

Baykov, A. A., Evtushenko, O. A., & Avaeva, S. M. (1988). A malachite green procedure for orthophosphate determination and its use in alkaline phosphatase-based enzyme immunoassay. *Analytical Biochemistry*, *171*(2). https://doi.org/10.1016/0003-2697(88)90484-8

Berg, J. M., Gatto, G. J., Stryer, L., & Tymoczko, J. L. (2015). *Biochemistry 8th Ed.*

Bhatia, S., & Goli, D. (2018). History, scope and development of biotechnology. In *Introduction to Pharmaceutical Biotechnology, Volume 1 - Basic techniques and concepts*. IOP Publishing. https://doi.org/10.1088/978-0-7503-1299-8ch1

Bisswanger, H. (2014). Enzyme assays. *Perspectives in Science*, *1*(1–6), 41–55. https://doi.org/10.1016/j.pisc.2014.02.005

Blankenship, R. (2002). *Molecular Mechanisms of Photosynthesis*.

Chan, W.-T., Verma, C. S., Lane, D. P., & Gan, S. K.-E. (2013). A comparison and optimization of methods and factors affecting the transformation of Escherichia coli. *Bioscience Reports*, *33*(6). https://doi.org/10.1042/BSR20130098

de Porcellinis, A. J., Nørgaard, H., Brey, L. M. F., Erstad, S. M., Jones, P. R., Heazlewood, J. L., & Sakuragi, Y. (2018). Overexpression of bifunctional fructose-1,6-bisphosphatase/sedoheptulose-1,7-bisphosphatase leads to enhanced photosynthesis and global reprogramming of carbon metabolism in Synechococcus sp. PCC 7002. *Metabolic Engineering*, *47*. https://doi.org/10.1016/j.ymben.2018.03.001

Durall, C., & Lindblad, P. (2015). Mechanisms of carbon fixation and engineering for increased carbon fixation in cyanobacteria. *Algal Research*, *11*. https://doi.org/10.1016/j.algal.2015.07.002

Feng, L., Sun, Y., Deng, H., Li, D., Wan, J., Wang, X., Wang, W., Liao, X., Ren, Y., & Hu, X. (2014). Structural and biochemical characterization of fructose-1,6/sedoheptulose-1,7-bisphosphatase from the cyanobacterium *Synechocystis* strain 6803. *FEBS Journal*, *281*(3). https://doi.org/10.1111/febs.12657

Friedlingstein, P., O'Sullivan, M., Jones, M. W., Andrew, R. M., Hauck, J., Olsen, A., Peters, G. P., Peters, W., Pongratz, J., Sitch, S., le Quéré, C., Canadell, J. G., Ciais, P., Jackson, R. B., Alin, S., Aragão, L. E. O. C., Arneth, A., Arora, V., Bates, N. R., … Zaehle, S. (2020). Global Carbon Budget 2020. *Earth System Science Data*, *12*(4). https://doi.org/10.5194/essd-12-3269-2020

Geladopoulos, T. P., Sotiroudis, T. G., & Evangelopoulos, A. E. (1991). A malachite green colorimetric assay for protein phosphatase activity. *Analytical Biochemistry*, *192*(1), 112–116. https://doi.org/10.1016/0003-2697(91)90194-X

Gong, F., Zhu, H., Zhang, Y., & Li, Y. (2018). Biological carbon fixation: From natural to synthetic. In *Journal of CO2 Utilization* (Vol. 28, pp. 221–227). Elsevier Ltd. https://doi.org/10.1016/j.jcou.2018.09.014

Gütle, D. D., Roret, T., Müller, S. J., Couturier, J., Lemaire, S. D., Hecker, A., Dhalleine, T., Buchanan, B. B., Reski, R., Einsle, O., Jacquot, J.-P., Balsera, M., Eklund, H., Raines, C. A., & Wolosiuk, R. A. (2016). Chloroplast FBPase and SBPase are thioredoxin-linked enzymes with similar architecture but different evolutionary histories. *PNAS*. https://doi.org/10.1073/pnas.1606241113

Hansen, J., Sato, M., Ruedy, R., Lo, K., Lea, D. W., & Medina-Elizade, M. (2006). *Global temperature change* (Vol. 103, Issue 39). www.pnas.orgcgidoi10.1073pnas.0606291103

Hu, X., Hui, D., Lingling, F., & Jian, W. (2011). *D-fructose 1,6-bisphosphatase class 2/sedoheptulose 1,7-bisphosphatase of Synechocystis sp. PCC 6803 in complex with FRUCTOSE-1,6-BISPHOSPHATE*.

Janasch, M., Asplund-Samuelsson, J., Steuer, R., & Hudson, E. P. (2018). Kinetic modeling of the Calvin cycle identifies flux control and stable metabolomes in *Synechocystis* carbon fixation. *Journal of Experimental Botany*. https://doi.org/10.1093/jxb/ery382

Jiang, Y.-H., Wang, D.-Y., & Wen, J.-F. (2012). The independent prokaryotic origins of eukaryotic fructose-1, 6-bisphosphatase and sedoheptulose-1, 7-bisphosphatase and the implications of their origins for the evolution of eukaryotic Calvin cycle. *BMC Evolutionary Biology*, *12*(1). https://doi.org/10.1186/1471-2148-12-208

Johnson, M. P. (2016). Photosynthesis. *Essays in Biochemistry*, *60*(3). https://doi.org/10.1042/EBC20160016

Knoot, C. J., Ungerer, J., Wangikar, P. P., & Pakrasi, H. B. (2018). Cyanobacteria: Promising biocatalysts for sustainable chemical production. *Journal of Biological Chemistry*, *293*(14). https://doi.org/10.1074/jbc.R117.815886

Lanzetta, P. A., Alvarez, L. J., Reinach, P. S., & Candia, O. A. (1979). An improved assay for nanomole amounts of inorganic phosphate. *Analytical Biochemistry*, *100*(1). https://doi.org/10.1016/0003-2697(79)90115-5

Liang, F., & Lindblad, P. (2016). Effects of overexpressing photosynthetic carbon flux control enzymes in the cyanobacterium Synechocystis PCC 6803. *Metabolic Engineering*, *38*. https://doi.org/10.1016/j.ymben.2016.06.005

Ma, W., Lanzhen, W., Wang, Q., Shi, D., & Chen, H. (2007). *Increased activity of the tandem fructose-1,6-bisphosphate aldolase, triosephosphate isomerase and fructose-1, 6-bisphosphatase enzymes in Anabaena sp. strain PCC 7120 stimulates photosynthetic yield*. https://doi.org/10.1007/s10811-007-9286-0

Nicholls, R. J. (2002). Rising sea levels: potential impacts and responses. In *Global Environment Change. (Issues in Environmental Science and Technology,* (pp. 83–107).

Pandolfi, J. M., Connolly, S. R., Marshall, D. J., & Cohen, A. L. (2011). Projecting Coral Reef Futures Under Global Warming and Ocean Acidification. *Science*, *333*(6041). https://doi.org/10.1126/science.1204794

Purich, D. (2010). *Enzyme Kinetics, Catalysis & Control: A Reference of Theory and Best-Practice Methods* (1st ed.). Elsevier.

Root, T. L., Price, J. T., Hall, K. R., Schneider, S. H., Rosenzweig, C., & Pounds, J. A. (2003). Fingerprints of global warming on wild animals and plants. *Nature*, *421*(6918). https://doi.org/10.1038/nature01333

Rosano, G. L., & Ceccarelli, E. A. (2014). Recombinant protein expression in Escherichia coli: advances and challenges. *Frontiers in Microbiology*, *5*. https://doi.org/10.3389/fmicb.2014.00172

Rosenzweig, C., Iglesias, A., Yang, X. B., Epstein, P. R., & Chivian, E. (2001). Climate Change and Extreme Weather Events; Implications for Food Production, Plant Diseases, and Pests. *Global Change and Human Health*, *2*(2). https://doi.org/10.1023/A:1015086831467

Rosgaard, L., de Porcellinis, A. J., Jacobsen, J. H., Frigaard, N. U., & Sakuragi, Y. (2012). Bioengineering of carbon fixation, biofuels, and biochemicals in

cyanobacteria and plants. *Journal of Biotechnology*, *162*(1), 134–147. https://doi.org/10.1016/j.jbiotec.2012.05.006

Rowlands, M. G., Newbatt, Y. M., Prodromou, C., Pearl, L. H., Workman, P., & Aherne, W. (2004). High-throughput screening assay for inhibitors of heat-shock protein 90 ATPase activity. *Analytical Biochemistry*, *327*(2). https://doi.org/10.1016/j.ab.2003.10.038

Soetaert, W., & Vandamm, E. (2006). The impact of industrial biotechnology. *Biotechnology Journal*. https://doi.org/10.1002/biot.200600066

Stott, P. (2016). How climate change affects extreme weather events. *Science*, *352*(6293). https://doi.org/10.1126/science.aaf7271

Sun, Y., Liao, X., Li, D., Feng, L., Li, J., Wang, X., Jin, J., Yi, F., Zhou, L., & Wan, J. (2012). Study on the interaction between cyanobacteria FBP/SBPase and metal ions. *Spectrochimica Acta Part A: Molecular and Biomolecular Spectroscopy*, *89*. https://doi.org/10.1016/j.saa.2011.12.014

Tamoi, M., Nagaoka, M., Miyagawa, Y., & Shigeoka, S. (2006). Contribution of Fructose-1,6-bisphosphatase and Sedoheptulose-1,7-bisphosphatase to the Photosynthetic Rate and Carbon Flow in the Calvin Cycle in Transgenic Plants. *Plant Cell Physiol*, *47*(3), 380–390. https://doi.org/10.1093/pcp/pcj004

United Nations. (2019). *World Population Prospects 2019 Volume II: Demographic Profiles*. Department of Economic and Social Affairs, Population Division.

Wang, D., Zhang, Y., Pohlmann, E. L., Li, J., & Roberts, G. P. (2011). The Poor Growth of Rhodospirillum rubrum Mutants Lacking RubisCO Is Due to the Accumulation of Ribulose-1,5-Bisphosphate. *Journal of Bacteriology*, *193*(13). https://doi.org/10.1128/JB.00265-11

Wilson, K., & Walker, J. M. (2018). *Principles and Techniques of Biochemistry and Molecular Biology* (A. Hofmann & S. Clokie, Eds.). Cambrdige University Press.

Zhou, X., & Arthur, G. (1992). Improved procedures for the determination of lipid phosphorus by malachite green. *Journal of Lipid Research*, *33*(8), 1233–1236. https://doi.org/10.1016/s0022-2275(20)40776-x

9. Appendix

Table A1

The genetic sequence for cloned WT and mutant cy-F/SBPase and used primers.

Name	Sequence
Wild type	GATTCGACCTTGGGGTTGGAAATCATCGAGGTAGTGGAGCAGGCTGCCATTGCTTCAGCCAAGTGGATGGGTAAAGGTGAAAAAAACACTGCGGATCAGGTCGCTGTCGAAGCTATGCGGGAGCGCATGAATAAAATCCACA TGCGGGGGCGCATTGTAATTGGTGAAGGGGAGCGCGATGATGCGCCGATGTTATATATCGGCGAAGAAGTAGGTATTTGCACTCGGGAAGATGCGAAGAGTTTTTGCAACCCAGATGAGCTCGTGGAGATCGACATCGCCGT AGACCCGTGCGAGGGGACAAACTTAGTCGCGTACGGCCAAAACGGGAGCATGGCAGTTCTTGCAATCAGCGAGAAAGGGGGCTTGTTCGCCGCGCCTGACTTTTACATGAAGAAACTGGCAGCTCCTCCAGCTGCTAAGGG GCACGTGGACATTGATAAAAGTGCGACAGAAAACTTAAAAATCTTGTCTGATTGCCTTAATCGTTCAATTGAAGAGTTGGTAGTGGTAGTTATGGATCGTCCTCGCCATAAAGAACTCATTCAGGAAATTCGTAATGCAGGGGCT CGTGTTCGCCTCATCTCTGACGGCGATGTTTCGGCTGCAATTTCGTGTGCTTTTTCGGGTACTAATATTCATGCCCTCATGGGCATCGGTGCTGCGCCAGAGGGTGTCATTTCTGCGGCTGCGATGCGCTGTCTTGGGGGGCA CTTTCAAGGGCAATTAATTTATGATCCTGAAGTTGTTAAAACGGGCTTAATCGGCGAGTCCCGGGAGGGTAATTTGGAACGTCTCGCGAGTATGGGTATCAAGAATCCGGACCAAGTCTATAACTGCGAGGAATTGGCTTGTGG TGAGACTGTTCTCTTTGCGGCTTGCGGCATCACTCCGGGGACGCTGATGGAGGGGGTTCGGTTTTTCACGGTGGTGTTCGGACTCAGAGTCTTGTGATCTCATCACAAAGCAGTACCGCACGGTTCGTGGATACCGTCCACA TGAAAGAATCGCCGAAAGTAATTCAACTCCAT
K29A	GATTCTACGCTGGGGTTAGAAATTATTGAAGTAGTTGAACAAGCAGCCATCGCCTCAGCGAAATGGATGGGTAAGGGGGAAGCAAATACAGCAGACCAAGTCGCTGTCGAGGCTATGCGGGAACGTATGAACAAGATTCACAT GCGTGGCCGCATCGTGATCGGTGAGGGCGAGCGCGATGATGCACCGATGTTATATATCGGTGAGGAGGTAGGGATCTGCACCCGCGAAGACGCAAAGTCTTTCTGCAACCCAGATGAACTGGTTGAAATCGACATCGCAGT CGACCCGTGTGAAGGTACTAACTTAGTCGCCTATGGGCAGAACGGCTCTATGGCCGTTTTAGCAATTTCGGAAAAAGGGGGTTTGTTCGCCGCGCCGGATTTTTATATGAAGAAGCTGGCGGCTCCGCCAGCAGCCAAAGGC CACGTGGACATTGATAAGAGCGCTACCGAGAATCTTAAAATTTTGTCCGATTGCTTGAATCGTAGCATTGAAGAGTTGGTGGTCGTTGTAATGGACCGCCCTCGGCATAAAGAACTCATTCAGGAGATTCGCAATGCAGGTGCG CGTGTTCGTTTGATTTCCGACGGTGACGTTTCGGCGGCCATCTCTTGCGCGTTCTCCGGGACCAATATCCATGCACTCATGGGCATCGGCGCTGCGCCTGAAGGGGTAATTAGTGCAGCCGCTATGCGTTGTCTTGGTGGCC ACTTCCAGGGGCAGCTTATCTATGACCCTGAAGTCGTTAAGACTGGGTTGATCGGCGAAAGTCGTGAGGGGAACCTTGAACGGCTCGCCAGCATGGGCATCAAGAATCCAGATCAAGTTTACAACTGCGAAGAACTTGCCTGT GGTGAAACGGTGCTTTTTGCAGCGTGCGGCATCACTCCAGGGACGCTGATGGAAGGTGTACGGTTTTTTCACGGGGGGGTTCGTACCCAATCCCTGGTCATCAGTTCGCAGAGCAGTACAGCTCGTTTTGTTGATACCGTCCA CATGAAAGAAAGCCCGAAGGTAATCCAGTTACAT
C75S	GATTCTACGTTGGGTCTGGAAATTATCGAAGTGGTGGAGCAAGCCGCCATTGCCAGCGCTAAATGGATGGGCAAAGGTGAAAAGAACACTGCGGATCAAGTAGCGGTCGAAGCGATGCGCGAGCGTATGAACAAAATCCACA TGCGTGGCCGTATTGTAATTGGCGAGGGGGAACGCGATGACGCCCCTATGCTGTACATTGGTGAGGAGGTGGGCATCTCCACGCGGGAGGATGCTAAAAGCTTCTGCAATCCGGATGAACTCGTAGAAATCGACATCGCAGT CGATCCTTGTGAAGGCACTAACCTGGTAGCTTATGGTCAGAACGGTTCAATGGCAGTACTGGCGATTTCGGAGAAGGGTGGGCTCTTTGCTGCCCCGGATTTTTATATGAAAAAGTTAGCAGCGCCACCAGCAGCTAAGGGTC ACGTTGATATTGATAAATCTGCAACAGAGAATTTAAAGATCCTGTCAGACTGTTTGAATCGGTCTATCGAGGAACTTGTGGTAGTCGTCATGGACCGCCCGCGGCATAAGGAGCTTATTCAGGAGATTCGCAACGCGGGGGCT CGCGTCCGTCTTATCAGTGATGGCGACGTCTCAGCCGCGATCTCATGCGCTTTTTCGGGGACCAACATCCATGCTTTGATGGGTATTGGTGCTGCGCCGGAAGGTGTAATTTCAGCCGCTGCAATGCGTTGCCTTGGTGGGC ACTTCCAGGGTCAGCTTATTTACGACCCTGAAGTGGTTAAAACCGGGTTAATCGGGGAATCCCGCGAAGGGAACCTGGAACGCTTGGCTTCTATGGGCATTAAAAACCCGGACCAGGTGTATAATTGTGAAGAGCTTGCTTGT GGTGAGACCGTCCTGTTTGCGGCCTGTGGCATCACGCCAGGGACGCTCATGGAAGGGGTGCGCTTTTTCCACGGCGGGGTTCGCACGCAATCGCTTGTGATCTCTTCTCAATCAAGCACCGCGCGCTTTGTAGATACCGTCC ACATGAAAGAATCGCCGAAGGTTATTCAGCTCCAT
T102A	GATTCAACATTAGGGTTAGAGATCATCGAGGTTGTGGAGCAGGCTGCGATTGCGTCTGCTAAGTGGATGGGTAAGGGCGAAAAAAACACAGCAGATCAGGTAGCAGTGGAAGCTATGCGTGAACGGATGAATAAAATCCACAT GCGTGGGCGGATTGTGATCGGGGAAGGGGAACGGGACGATGCACCTATGTTGTACATCGGGGAGGAGGTCGGCATCTGCACGCGGGAAGACGCGAAGTCTTTTTGTAATCCTGATGAATTAGTGGAAATTGACATCGCAGT GGACCCGTGTGAAGGTGCGAACTTGGTAGCTTACGGTCAGAATGGGTCAATGGCCGTTCTGGCTATCTCCGAGAAAGGGGGTTTATTTGCCGCACCAGATTTCTACATGAAAAAGCTCGCAGCACCGCCTGCGGCCAAGGGG CACGTTGATATTGACAAGAGTGCGACAGAAAATCTTAAGATCTTGAGCGACTGCTTGAATCGCTCAATTGAGGAGCTCGTCGTTGTAGTTATGGATCGTCCTCGTCATAAGGAACTGATCCAAGAGATCCGTAATGCAGGCGCT CGTGTGCGCCTTATTAGTGACGGCGATGTCAGTGCGGCTATTAGTTGTGCATTCAGCGGGACCAATATTCATGCGTTAATGGGTATTGGTGCGGCTCCAGAGGGCGTAATTTCCGCCGCCGCGATGCGCTGCCTTGGCGGGC ACTTTCAGGGGCAATTAATTTACGATCCTGAGGTAGTCAAAACCGGCCTCATCGGTGAGTCGCGGGAGGGTAACTTGGAGCGTCTCGCTTCAATGGGCATCAAAAATCCTGACCAGGTTTATAACTGTGAAGAACTTGCATGC GGGGAAACGGTCTTATTCGCAGCTTGTGGGATTACTCCTGGGACCTTGATGGAGGGGGTGCGTTTCTTTCATGGCGGCGTTCGTACCCAGTCGCTTGTCATCTCTAGTCAAAGTTCAACTGCTCGTTTTGTAGATACAGTCCAC ATGAAAGAATCTCCGAAAGTCATTCAATTGCAT
K134A	GATAGTACTCTTGGTTTAGAAATTATCGAAGTGGTGGAACAGGCTGCAATCGCGAGTGCCAAGTGGATGGGTAAAGGCGAAAAGAATACGGCAGATCAAGTTGCAGTAGAAGCCATGCGTGAACGGATGAACAAGATTCACAT GCGTGGGCGGATTGTCATTGGCGAAGGTGAACGTGATGATGCTCCGATGCTCTACATCGGCGAGGAAGTCGGCATTTGTACCCGTGAGGATGCGAAGAGTTTTTGCAATCCAGATGAATTAGTTGAGATCGACATCGCAGTG GATCCTTGCGAGGGTACAAACCTGGTTGCGTATGGCCAAAACGGTAGTATGGCGGTCCTTGCGATCTCTGAGAAGGGTGGCCTCTTTGCCGCACCAGACTTCTACATGAAAGCCTTGGCGGCACCGCCAGCGGCGAAGGGG CATGTAGATATTGACAAATCCGCTACTGAAAATTTGAAAATCCTGTCCGATTGTCTGAACCGGAGCATCGAAGAGCTCGTTGTTGTAGTGATGGACCGGCCTCGGCACAAAGAACTCATTCAAGAGATTCGTAATGCGGGCGCA CGTGTCCGTCTCATTTCGGACGGTGATGTGTCTGCGGCTATTAGCTGCGCGTTCAGTGGTACAAATATCCACGCTCTGATGGGCATCGGCGCTGCTCCAGAGGGGGTTATCTCCGCAGCAGCTATGCGGTGCTTAGGTGGCC ACTTCCAAGGCCAGCTCATCTACGATCCGGAGGTCGTAAAGACTGGTCTTATTGGGGAGAGCCGTGAGGGGAATCTGGAGCGTTTAGCCTCGATGGGTATCAAAAATCCGGACCAAGTGTATAATTGTGAAGAACTTGCTTGT GGCGAGACAGTGCTCTTCGCGGCTTGTGGGATCACGCCTGGGACGCTTATGGAAGGCGTACGTTTCTTTCACGGTGGTGTCCGCACCCAATCTTTGGTGATCAGTTCTCAGTCGTCCACTGCTCGCTTTGTGGATACCGTTCA CATGAAGGAGAGCCCTAAGGTTATCCAACTGCAT
R176A	GATTCCACGCTCGGCTTAGAGATCATTGAGGTAGTGGAGCAAGCCGCAATTGCAAGTGCAAAATGGATGGGGAAGGGCGAAAAAAACACTGCGGACCAAGTTGCAGTGGAAGCCATGCGTGAACGTATGAACAAAATCCACA TGCGGGGTCGCATTGTGATTGGTGAAGGTGAGCGCGACGATGCACCTATGCTCTATATTGGTGAAGAAGTTGGGATCTGCACGCGGGAGGATGCTAAGTCCTTTTGTAATCCAGACGAATTGGTAGAAATTGACATTGCGGTT GACCCTTGTGAAGGGACCAATCTTGTCGCGTATGGGCAGAACGGTTCTATGGCTGTGTTGGCTATTTCTGAAAAGGGGGGCCTCTTTGCTGCTCCAGATTTCTACATGAAAAAGCTGGCAGCACCGCCGGCGGCTAAGGGTC ATGTGGACATCGACAAAAGCGCCACTGAAAATTTGAAGATTTTGTCCGACTGCCTGAACCGCTCGATCGAGGAACTCGTTGTCGTCGTAATGGACGCTCCACGGCACAAAGAGCTTATTCAGGAAATTCGGAACGCAGGCGCA CGCGTCCGTCTTATCAGTGATGGCGACGTGAGTGCGGCAATTTCCTGTGCATTCAGTGGCACGAACATTCACGCCCTCATGGGGATCGGTGCAGCTCCAGAGGGCGTGATCTCTGCAGCCGCCATGCGGTGCTTAGGTGGT CACTTCCAAGGCCAGTTGATTTATGACCCGGAGGTTGTGAAAACTGGCCTGATCGGGGAGTCCCGCGAGGGCAATCTGGAGCGGCTCGCTTCGATGGGGATTAAAAACCCAGATCAGGTTTATAACTGTGAGGAGCTGGCAT GCGGGGAAACAGTTCTCTTCGCTGCATGCGGTATTACTCCAGGCACGCTCATGGAGGGTGTACGGTTCTTCCACGGTGGCGTCCGGACGCAATCGCTTGTGATCTCGTCGCAATCAAGTACCGCGCGGTTCGTAGATACGGT GCACATGAAAGAGTCGCCAAAGGTTATTCAATTGCAT
R307A	GATTCAACACTCGGCCTTGAGATTATCGAAGTGGTAGAGCAAGCTGCGATTGCTTCAGCCAAGTGGATGGGCAAAGGGGAGAAAAATACGGCCGACCAGGTAGCCGTTGAGGCAATGCGTGAGCGTATGAACAAGATCCACA TGCGGGGCCGGATCGTTATTGGGGAAGGCGAGCGTGATGATGCACCGATGCTCTATATCGGCGAGGAGGTTGGGATCTGTACACGCGAGGATGCCAAGAGTTTTTGCAATCCAGACGAACTTGTGGAGATTGATATTGCAGT TGACCCATGCGAAGGTACAAATCTGGTGGCTTATGGTCAAAATGGTTCAATGGCGGTCCTTGCTATTAGCGAGAAGGGGGGGCTGTTCGCCGCGCCAGATTTTTACATGAAAAAGCTCGCTGCTCCGCCGGCGGCAAAAGGG CACGTTGACATTGACAAGTCCGCCACTGAAAATTTGAAGATTTTGAGTGACTGTTTAAATCGTTCTATCGAAGAGTTGGTCGTAGTAGTGATGGATCGTCCGCGCCACAAGGAACTGATCCAAGAGATTCGCAATGCAGGCGCT CGTGTACGTTTAATTTCAGATGGGGATGTCTCGGCAGCGATCTCCTGCGCATTTTCCGGTACAAACATCCACGCACTTATGGGGATTGGGGCCGCGCCGGAGGGCGTGATCTCGGCGGCAGCGATGCGCTGCCTTGGTGGT CACTTCCAGGGTCAACTTATCTACGATCCGGAGGTAGTGAAAACCGGGCTCATTGGCGAAAGTCGTGAGGGTAATTTGGAACGCCTCGCGAGTATGGGCATTAAAAACCCGGATCAAGTGTACAACTGCGAGGAGTTGGCTT GCGGCGAAACTGTGCTCTTTGCGGCGTGCGGTATTACTCCTGGTACCCTTATGGAAGGGGTAGCGTTTTTCCATGGTGGGGTACGGACGCAATCTCTTGTTATCTCGTCGCAATCGTCAACAGCCCGGTTCGTCGACACCGTT CACATGAAAGAATCTCCAAAGGTGATCCAATTGCAT
G25A	GATTCCACGCTCGGTTTGGAAATCATCGAAGTCGTTGAGCAAGCAGCGATTGCGAGTGCGAAGTGGATGGCAAAGGGCGAGAAGAATACTGCCGATCAGGTGGCTGTAGAAGCAATGCGGGAGCGCATGAACAAAATTCACA TGCGTGGCCGGATTGTTATTGGTGAAGGCGAGCGGGATGACGCACCTATGCTGTATATTGGTGAGGAGGTAGGGATTTGCACTCGGGAAGATGCGAAGTCATTCTGCAACCCTGACGAACTCGTCGAGATCGATATCGCAGT TGACCCATGCGAGGGCACAAACCTGGTCGCCTACGGTCAAAACGGGTCAATGGCAGTTTTGGCTATTTCAGAAAAAGGCGGTCTTTTCGCGGCCCCGGATTTTTACATGAAAAAGCTTGCTGCTCCACCTGCCGCTAAGGGCC ACGTCGACATCGACAAATCGGCCACAGAGAACCTCAAAATTCTGAGTGACTGCCTCAATCGGTCGATCGAGGAATTAGTTGTTGTTGTCATGGACCGTCCTCGGCATAAGGAATTGATCCAGGAGATCCGGAATGCGGGGGCT CGGGTGCGGTTGATTTCTGACGGTGATGTGTCAGCCGCTATCTCGTGCGCGTTTTCAGGCACCAATATTCACGCACTTATGGGGATCGGGGCCGCGCCTGAGGGGGTGATCAGCGCCGCGGCCATGCGCTGTTTGGGCGGG CATTTCCAAGGTCAGCTGATCTACGACCCTGAAGTCGTTAAGACTGGGCTGATCGGGGAGAGTCGCGAAGGGAATCTTGAGCGGCTCGCTTCTATGGGGATTAAGAATCCGGATCAAGTATATAATTGTGAAGAATTAGCGTG CGGGGAGACAGTATTATTTGCAGCGTGCGGGATTACGCCGGGGACACTTATGGAGGGGGTTCGGTTTTTCCACGGGGGGGTCCGTACCCAATCTCTCGTAATTAGCTCGCAGTCCAGCACGGCCCGGTTCGTTGATACGGTC CACATGAAAGAATCGCCAAAGGTCATTCAACTGCAT
K134N	CATATGGACTCGACTCTTGGTCTTGAGATTATCGAAGTCGTCGAACAAGCTGCGATCGCTTCGGCTAAGTGGATGGGCAAAGGTGAAAAAAACACCGCAGACCAAGTCGCTGTCGAGGCAATGCGGGAACGTATGAATAAGAT TCACATGCGCGGGCGTATCGTCATTGGTGAAGGCGAGCGTGATGACGCTCCAATGTTATACATCGGTGAAGAAGTGGGGATTTGCACTCGCGAAGACGCGAAATCTTTCTGCAACCCAGACGAATTAGTTGAGATCGATATTG CTGTAGATCCGTGTGAGGGTACCAATTTGGTAGCATACGGTCAGAATGGCAGCATGGCCGTTTTAGCGATCTCTGAGAAGGGCGGTTTGTTTGCAGCTCCTGATTTTTATATGAAAAACCTTGCGGCCCCACCGGCGGCTAAA GGCCATGTGGACATTGACAAGAGTGCTACTGAGAATTTGAAAATCCTTTCAGATTGTCTTAATCGTAGCATTGAGGAATTAGTTGTGGTCGTCATGGACCGTCCTCGTCATAAGGAACTTATTCAAGAGATCCGTAACGCTGGG GCCCGCGTTCGGTTAATTTCCGACGGGGACGTCTCAGCCGCCATTAGCTGTGCGTTTTCCGGCACGAACATCCATGCTTTAATGGGGATTGGTGCTGCACCTGAGGGGGTGATCTCAGCAGCAGCGATGCGCTGCTTGGGTG GGCACTTTCAAGGTCAACTTATTTATGACCCAGAGGTCGTCAAAACTGGTTTGATCGGTGAAAGTCGTGAGGGGAATCTCGAACGCCTTGCCTCCATGGGCATCAAGAACCCAGATCAGGTCTATAACTGCGAGGAATTGGCG TGCGGTGAGACAGTTCTGTTTGCAGCGTGTGGGATTACCCCTGGCACGCTGATGGAAGGTGTACGCTTTTTTCATGGTGGGGTACGGACCCAGTCACTCGTTATCTCCAGCCAGTCGTCCACAGCGCGGTTTGTTGACACGG TACACATGAAAGAATCACCTAAAGTGATTCAACTTCATTAATACGCTCGAG
P138A	CATATGGACTCCACATTAGGCCTTGAGATCATCGAGGTAGTGGAACAAGCAGCCATCGCGAGCGCGAAATGGATGGGCAAGGGTGAGAAGAATACTGCGGACCAAGTAGCAGTGGAGGCCATGCGGGAACGCATGAACAAA ATTCACATGCGGGGCCGTATCGTAATTGGTGAGGGTGAGCGGGACGACGCCCCAATGCTCTATATTGGTGAAGAAGTAGGCATCTGCACACGGGAAGACGCGAAAAGCTTCTGTAACCCGGATGAGTTAGTTGAGATCGACA TCGCAGTAGACCCATGTGAAGGGACAAATCTCGTTGCCTACGGCCAAAATGGGTCTATGGCAGTCCTCGCCATCTCCGAGAAAGGCGGTCTTTTCGCAGCGCCAGACTTTTATATGAAGAAACTGGCAGCTGCTCCGGCCGC AAAAGGCCATGTCGACATCGATAAGAGCGCAACCGAGAACCTTAAGATTTTGTCAGACTGCCTTAATCGTAGTATTGAGGAGTTAGTGGTAGTCGTCATGGATCGCCCTCGTCATAAGGAGCTCATCCAAGAGATCCGCAACG CCGGTGCCCGTGTACGTCTGATCTCGGACGGGGATGTATCGGCTGCTATTAGCTGCGCTTTCTCCGGGACAAATATCCACGCATTGATGGGGATTGGCGCCGCGCCGGAGGGCGTCATTAGCGCCGCTGCGATGCGCTGTC TCGGGGGGCATTTTCAAGGTCAACTCATCTATGACCCTGAGGTTGTTAAGACAGGTCTGATCGGCGAGTCGCGCGAAGGCAACTTGGAGCGTCTGGCTTCAATGGGGATCAAGAATCCTGACCAAGTTTACAATTGTGAGGAG TTAGCGTGTGGCGAAACAGTTTTATTCGCCGCCTGTGGCATCACTCCAGGGACGTTAATGGAAGGTGTACGCTTTTTCCACGGCGGGGTTCGGACGCAATCTCTGGTTATTAGTAGCCAGTCTTCCACAGCGCGTTTCGTCGA CACCGTACACATGAAAGAGTCGCCTAAAGTAATCCAATTACATTAATACGCTCGAG
R192N	CATATGGACTCGACGCTCGGGCTTGAGATTATCGAAGTGGTGGAACAAGCTGCCATTGCTAGCGCGAAGTGGATGGGTAAGGGCGAAAAAAATACGGCTGACCAGGTTGCGGTGGAGGCCATGCGTGAACGCATGAATAAG ATCCACATGCGGGGGCGTATCGTAATCGGCGAAGGCGAGCGGGACGACGCTCCGATGTTGTATATTGGGGAGGAGGTTGGCATTTGTACTCGTGAGGACGCAAAAAGCTTCTGCAATCCTGATGAGCTGGTGGAGATCGATA TTGCTGTAGACCCGTGCGAGGGTACTAATCTTGTGGCATACGGTCAGAATGGGTCAATGGCGGTACTCGCAATCTCAGAGAAAGGTGGGCTCTTCGCTGCCCCTGACTTCTACATGAAAAAGCTGGCAGCACCTCCGGCAGC CAAGGGGCACGTTGACATCGACAAGAGCGCGACCGAAAACCTCAAGATCCTCAGCGATTGCCTCAACCGCTCGATTGAGGAACTGGTGGTAGTCGTTATGGATCGTCCTCGCCATAAGGAACTCATTCAAGAGATCCGCAAT GCCGGCGCGAACGTACGGTTAATTAGCGATGGTGACGTTTCGGCAGCCATTTCTTGTGCTTTTTCGGGGACTAATATTCACGCCCTCATGGGGATCGGCGCGGCGCCTGAAGGGGTCATTTCTGCTGCCGCCATGCGTTGTC TGGGGGGGCATTTCCAAGGTCAGCTGATTTATGACCCTGAAGTGGTAAAGACTGGCCTTATTGGCGAGAGCCGCGAGGGTAATTTAGAGCGTCTGGCTTCTATGGGTATCAAGAACCCAGACCAAGTGTACAACTGCGAGGA ATTAGCGTGCGGGGAAACGGTTCTTTTTGCAGCGTGCGGTATTACTCCGGGGACGCTCATGGAAGGGGTACGCTTCTTCCATGGCGGCGTGCGTACACAAAGCCTCGTTATTTCCTCACAATCGTCAACGGCCCGGTTCGTA GATACGGTACACATGAAGGAGAGCCCTAAAGTTATCCAACTGCATTAATACGCTCGAG
R194H	CATATGGACTCAACTCTCGGTCTTGAGATTATCGAAGTAGTTGAACAGGCTGCAATTGCAAGCGCTAAGTGGATGGGGAAGGGGGAAAAGAACACCGCTGACCAGGTCGCAGTGGAAGCCATGCGCGAGCGTATGAATAAAA TCCACATGCGTGGTCGCATTGTAATTGGGGAGGGCGAGCGGGATGACGCGCCAATGCTGTATATCGGTGAAGAGGTTGGGATCTGTACCCGCGAAGACGCAAAATCTTTCTGCAACCCGGATGAGTTGGTAGAAATTGACAT CGCAGTCGACCCTTGTGAGGGCACAAACTTGGTCGCCTATGGGCAGAATGGTTCGATGGCGGTCCTTGCGATCTCTGAGAAGGGTGGTCTCTTTGCAGCTCCAGACTTTTATATGAAGAAGCTCGCGGCTCCACCAGCAGCT AAGGGTCATGTGGACATCGATAAGTCAGCAACCGAAAATCTGAAGATTCTGTCAGATTGCCTCAATCGCTCAATTGAGGAATTAGTCGTGGTCGTTATGGACCGCCCTCGTCATAAGGAGTTAATTCAAGAAATTCGCAATGCT GGGGCACGGGTCCATTTGATTTCTGACGGTGACGTGTCCGCTGCCATCAGCTGTGCGTTCAGCGGGACAAACATTCATGCTTTGATGGGGATCGGGGCGGCCCCAGAGGGTGTGATCTCTGCCGCCGCGATGCGTTGCCTT GGTGGCCATTTTCAGGGCCAACTCATCTACGATCCGGAAGTTGTAAAAACAGGGCTGATTGGCGAAAGTCGTGAGGGGAACCTGGAGCGGCTTGCGTCAATGGGCATTAAAAATCCAGACCAGGTATACAATTGCGAGGAGC TGGCATGCGGTGAAACTGTGCTCTTTGCAGCATGCGGTATCACACCTGGCACACTTATGGAGGGCGTACGTTTCTTTCATGGGGGTGTCCGTACCCAGTCGTTAGTCATCTCGTCTCAATCCTCCACAGCACGCTTCGTAGATA CGGTACACATGAAGGAGAGCCCTAAGGTCATCCAATTGCATTAATACGCTCGAG
A216V	CATATGGACAGCACGTTAGGGCTGGAGATTATCGAGGTTGTCGAGCAAGCTGCCATTGCTAGTGCCAAGTGGATGGGCAAAGGCGAAAAAAATACTGCAGATCAAGTAGCCGTGGAGGCGATGCGCGAACGGATGAACAAAA TTCACATGCGCGGTCGGATCGTTATTGGTGAAGGCGAGCGTGACGACGCACCTATGCTGTATATCGGGGAAGAGGTTGGTATTTGCACGCGGGAGGATGCTAAGAGTTTTTGCAACCCAGACGAGCTTGTTGAAATCGACAT CGCGGTTGATCCTTGCGAAGGTACTAACCTTGTTGCGTACGGGCAGAACGGGTCTATGGCGGTCTTGGCAATCAGCGAAAAAGGCGGGTTATTTGCTGCCCCTGATTTCTACATGAAGAAGTTAGCCGCTCCACCTGCAGCG AAGGGTCACGTCGATATCGACAAATCCGCTACTGAGAACCTGAAAATCCTGTCCGATTGTCTTAACCGCAGCATCGAGGAATTAGTGGTCGTGGTAATGGATCGTCCACGGCACAAGGAACTCATCCAGGAAATTCGCAACGC AGGTGCACGTGTCCGTCTGATTAGCGATGGGGACGTTTCTGCGGCTATTTCCTGTGCCTTTTCCGGTACTAATATCCATGTATTGATGGGCATCGGGGCTGCACCGGAGGGGGTTATTTCGGCGGCGGCCATGCGCTGCCTC GGTGGGCATTTTCAGGGTCAACTTATTTATGATCCTGAAGTGGTAAAGACCGGCCTTATTGGCGAAAGTCGCGAAGGTAATTTGGAGCGCCTCGCTTCCATGGGTATCAAAAACCCAGATCAGGTCTATAATTGCGAGGAACTG GCCTGTGGCGAAACGGTACTCTTTGCCGCTTGTGGGATTACGCCGGGGACGTTAATGGAGGGGGTTCGCTTTTTTCACGGCGGTGTACGGACACAATCTCTTGTAATTTCATCTCAATCATCCACAGCCCGTTTTGTAGACACA GTTCACATGAAGGAGAGCCCAAAGGTTATTCAACTCCACTAATACGCTCGAG
M218I	CATATGGATTCCACCCTCGGTCTGGAGATCATTGAAGTTGTCGAGCAGGCGGCTATTGCTTCAGCAAAGTGGATGGGCAAAGGGGAGAAAAATACTGCAGATCAAGTCGCCGTTGAGGCCATGCGCGAGCGGATGAACAAGA TCCACATGCGGGGGCGTATCGTCATTGGTGAGGGCGAGCGTGACGACGCTCCAATGTTATATATTGGTGAGGAGGTGGGGATCTGTACACGGGAGGACGCAAAATCTTTCTGCAACCCTGACGAGCTGGTAGAGATTGACAT CGCGGTCGATCCGTGCGAAGGCACTAACCTCGTGGCCTACGGCCAAAACGGGAGCATGGCCGTGCTGGCAATCTCCGAGAAGGGGGGCTTATTTGCAGCACCTGACTTTTACATGAAAAAGTTGGCTGCGCCGCCGGCGGC GAAGGGGCATGTGGACATCGATAAGTCAGCTACTGAGAACCTGAAAATTCTGAGTGATTGTCTTAATCGCAGCATTGAGGAGCTGGTGGTGGTCGTTATGGACCGCCCTCGGCATAAGGAATTGATTCAAGAGATTCGGAACG CAGGGGCCCGGGTCCGGTTGATTAGTGACGGCGACGTAAGCGCGGCAATCTCGTGCGCTTTCTCAGGTACTAACATCCATGCACTCATTGGGATCGGTGCGGCGCCGGAGGGCGTAATCAGTGCGGCTGCCATGCGTTGTC TTGGCGGTCACTTTCAAGGGCAACTCATCTACGATCCTGAAGTCGTAAAGACAGGTTTGATCGGGGAATCACGGGAAGGTAACCTTGAGCGCCTGGCGTCAATGGGGATTAAAAACCCTGACCAGGTTTACAACTGTGAAGAA CTTGCCTGCGGTGAAACGGTTCTGTTCGCAGCCTGTGGTATTACACCTGGTACTCTGATGGAGGGGGTCCGTTTTTCCACGGCGGTGTCCGCACTCAGTCGCTTGTTATCAGTAGCCAATCTAGTACAGCCCGCTTCGTCGA TACTGTCCACATGAAGGAATCTCCTAAGGTCATTCAATTACATTAATACGCTCGAG

G219V	CATATGGATTCTACCTTGGGCCTTGAGATCATTGAGGTAGTTGAACAAGCAGCAATCGCATCGGCGAAGTGGATGGGTAAAGGCGAAAAGAATACAGCGGATCAGGTTGCCGTCGAAGCCATGCGCGAACGGATGAACAAAA TCCACATGCGGGGTCGGATTGTAATTGGCGAGGGCGAACGGGACGATGCTCCAATGCTCTACATTGGCGAAGAGGTTGGTATTTGTACACGGGAGGACGCAAAGTCTTTTTGTAACCCGGATGAACTCGTGGAGATCGACAT TGCCGTAGATCCGTGTGAAGGCACGAACCTTGTAGCGTATGGTCAAAACGGCTCCATGGCTGTGTTGGCTATTTCTGAGAAGGGGGGTCTTTTCGCGGCCCCGGATTTCTACATGAAAAAATTGGCCGCGCCACCTGCAGCG AAAGGCCATGTAGACATTGATAAAAGCGCGACGGAGAACTTAAAGATCCTCTCGGACTGTCTTAATCGGTCAATCGAAGAACTCGTCGTGGTTGTGATGGACCGCCCACGTCATAAGGAGTTGATCCAGGAGATTCGGAACGC AGGGGCACGTGTTCGCCTTATTTCAGATGGCGATGTTTCGGCCGCAATCTCTTGCGCTTTCTCGGGGCACGAACATCCACGCACTGATGGTGATCGGGGCTGCCCCTGAAGGGGTGATTAGCGCAGCCGCGATGCGGTGCCT CGGGGGTCATTTTCAGGGCCAATTAATTTATGACCCAGAAGTGGTGAAGACGGGGTTAATCGGGGAAAGTCGGGAAGGGAACCTGGAGCGCCTGGCTAGTATGGGGATCAAGAACCCGGACCAGGTATATAACTGTGAAGA GCTTGCATGTGGGGAAACCGTCCTTTTTGCTGCCTGTGGTATTACTCCTGGCACCCTTATGGAAGGCGTTCGTTTCTTTCACGGTGGGGTACGTACCCAGTCACTTGTTATCAGTTCCCAATCTAGCACTGCTCGTTTCGTAGAT ACGGTGCACATGAAGGAATCCCCTAAAGTTATTCAGTTGCATTAATACGCTCGAG
Forward primer	CCATTCCGCCTGACCTCATATG
Reverse primer	CACTGAGCCTCCACCTAG
Sequencing primer	GCTAGTTATTGCTCAGCGG

Table A2

A comprehensive overview of the reaction components in the colorimetric assay

Assay components in 96-well plate			
Name	**Components**	**Volume per well (µL)**	**Role**
Assay buffer	• 50 mM Tris-HCl pH 8, • 15 mM $MgCl_2$	100	The assay buffer acts as a dilutant for the development solution.
Development solution	• 1.20 g/L MG-$C_2H_2O_4$ salt • 1.75 g/L $(NH_4)_6Mo_7O_{24}{\cdot}4H_2O$ • 0.21% v/v Tween20 (Polysorbate 20) • Filtered with a 0.2 µm filter	36	This solution was used to quench the sample from the enzyme reaction as well as forming the MG-Molybdate-Pi complex that was measured spectrophotometrically.
Citrate	• 34% w/v $C_6H_9Na_3O_9$	7.5	Added to each well after every sample from the enzyme reaction to give a more stable color development.
Reaction buffer and substrate solution			
Name	**Components**	**Role**	
Reaction buffer	• 50 mM Tris-HCl pH 8, • 15 mM $MgCl_2$ • 10 mM DTT	The buffer which the enzymatic reaction is diluted in.	
Substrate solution	• 0.1-5mM fructose 1.6-bisphosphate (FBP) diluted in reaction buffer	The substrate was added to each reaction according to the explanation for "Enzyme reaction" below. Six different FBP stock solutions of 0.1, 0.25, 0.5, 1, 2.5 and 5 mM were prepared.	
Enzyme reaction, Pi standards and blank			
Name	**Components**	**Preparation**	**Role**
Enzyme reaction	• 0.91 µg/ml purified cy-F/SBPase enzyme diluted in reaction buffer. • Substrate solution	Each enzyme reaction was diluted in 1 part 0.91 µg/ml enzyme and 9 parts substrate solution. The resulting working concentrations was 0.819 µg/ml enzyme and 0.01-0.05 mM FBP. The total reaction volume was 90 µL.	Prior to the addition of substrate, the enzyme reaction got to pre-incubate for 10 min at 30°C. The enzyme reactions were prepared in duplicates and were sampled at different timepoints based on the type of experiment. At each time point, 20 µL of enzyme reaction was taken and added to the development solution in the 96-well plate. Citrate was then added to the well.
P_i standards	• 0-100 mM $Na_2HPO_4{\cdot}2H_2O$ diluted in reaction buffer	The P_i standards were diluted in reaction buffer. 11 standard concentrations of 2.19, 3.13, 4.38, 6.25, 8.75, 12.5, 17.5, 25, 35, 50 and 100 µM were prepared.	20 µL of each P_i standard was added to the development solution in separate wells along with citrate.
Blank	• Reaction buffer	See "Reaction buffer" for preparation. A tube containing only reaction buffer was incubated in parallel with the enzyme reactions. The absorbance from this sample was then subtracted from the absorbance measurements of the enzyme reaction to calibrate for background signal.	